Evidence of abrupt climate change at 9.3 ka and 8.2 ka in the central Canadian Arctic: Connection to the North Atlantic and Atlantic Meridional Overturning Circulation

David F. Porinchu [a, *], Glen M. MacDonald [b], Katrina A. Moser [c], Nicolas Rolland [d], Konstantin Kremenetski [b], Heikki Seppä [e], Kathleen M. Rühland [f]

[a] Department of Geography, University of Georgia, Athens, GA 30602, USA
[b] Departments of Geography and EEB, UCLA, Los Angeles, CA 90095, USA
[c] Department of Geography, The University of Western Ontario, London, ON N6A 5C2, Canada
[d] Fisheries and Oceans Canada, Moncton, NB, E1C 5K4, Canada
[e] Department of Geosciences and Geography, University of Helsinki, Finland
[f] PEARL, Department of Biology, Queen's University, Kingston, ON K7L 3N6, Canada

ARTICLE INFO

ABSTRACT

This study presents the results of a multi-proxy analysis of a Holocene lacustrine sediment sequence recovered from a small tundra lake in the central Canadian Arctic and links climatic variations there to the North Atlantic. Chironomid and pollen-based reconstructions of mean July air temperature (MJAT) document notable deviations at 9.3 ka and 8.2 ka. Chironomid-inferred July air temperature is depressed by 1.4 °C at 9.3 ka and 1.7 °C at 8.2 ka relative to the long-term chironomid-inferred Holocene average of 9.4 °C. These cooling events also correspond to an increase in Gramineae (Poaceae) and a decrease in *Betula* pollen, reflecting a decrease in the density of dwarf birch cover. Concurrent, abrupt increases in several diatom taxa, including aerophilic epiphytes, and *Sphagnum* indicate an expansion of moss habitats as a result of wetter conditions. The expression and timing of the cooling evidenced at TK2 during the early Holocene is consistent with abrupt climate events identified in the North Atlantic and coincides with intervals of North Atlantic cooling and weakened Atlantic Meridional Overturning Circulation (AMOC). This research, which improves our understanding of the spatial extent and magnitude of the 9.3 ka and 8.2 ka events in the central Canadian Arctic, serves as a benchmark for coupled-ocean atmosphere climate models simulating the response of the climate system to abrupt climate events and provides insight in marine-atmosphere teleconnections in the circum-North Atlantic region.

© 2019 Elsevier Ltd. All rights reserved.

1. Introduction

Observational and modeling studies have demonstrated that the circum-Arctic is experiencing large positive deviations in thermal conditions relative to historic climatology and the most recent climate normal period (1981–2010) (see IPCC, 2013). These studies have revealed that Arctic environments have been experiencing rapid warming and environmental changes in recent decades driven by greenhouse gas radiative forcing and associated feedback mechanisms, such as the reduction of sea-ice albedo (Flanner et al.,

2011) and altered geochemical cycles (Romanovsky et al., 2002; Frey and McClelland, 2009). Decadal- and multi-decadal variability in the Arctic climate system is also influenced by conditions in the North Atlantic including variations in Atlantic meridional overturning circulation (AMOC), a key component of global circulation (Delworth and Zeng, 2016). AMOC is influenced by temperature and salinity, and in turn strongly influences the distribution of heat and freshwater transport on multi-decadal timescales with weak (strong) AMOC associated with a cooler (warmer) North Atlantic (Jackson et al., 2015). AMOC has the potential to influence conditions widely in the Arctic and beyond (Rahmstorf, 2002; Morrill et al., 2013; Buckley and Marshall, 2016; Delworth and Zeng, 2016). AMOC has weakened in recent years (Thornalley et al.,

2018) and has been predicted to weaken through the 21st century in response to anthropogenic climate change as surface waters of the North Atlantic warm, freshen, and become less dense (IPCC, 2013). However, the response of AMOC in coming decades (Drijfhout, 2015; Rind et al., 2018), and how this response will affect areas such as the Arctic, remains a major source of uncertainty in climate projections (Rahmstorf et al., 2015; Liu et al., 2017).

Research focusing on the influence of AMOC on the contemporary Arctic climate system has highlighted the importance of using the paleo-record to document how past changes in AMOC influenced the Arctic climate system (Hansen et al., 2016). Climate variability during the Pleistocene-Holocene transition in the Arctic and circum-North Atlantic regions has been linked to changes in North Atlantic salinity and temperature conditions and resulting fluctuations in the strength of AMOC (Bond et al., 2001; Clark et al., 2001; Hou et al., 2012). The early Holocene (~12 ka − 8 ka) was characterized by enhanced summer insolation at high northern latitudes (Berger and Loutre, 1991), the continued retreat and eventual collapse of the Laurentide Ice Sheet (Dyke et al., 2002), and a rapid, time-transgressive increase in near surface temperature (Kaufman et al., 2004, 2016; Briner et al., 2016). However, the increase in near surface temperature observed during the early Holocene was perturbed by a series of abrupt climate events, the most pronounced of which occurred at ~9.3 ka (Fleitmann et al., 2008; Axford et al., 2009; Yu et al., 2010; Gavin et al., 2011; Hou et al., 2012) and 8.2 ka (Alley et al., 1997; Clark et al., 2001; Morrill and Jacobsen, 2005; Daley et al., 2009; Morrill et al., 2013; Liu et al., 2013). Although the geographical extent of these events is not well resolved, similarities in the temporal and spatial pattern of the climate anomalies associated with these events suggest a common forcing or trigger (Barber et al., 1999; Yu et al., 2010), such as episodic weakening of AMOC due to increased freshwater fluxes (Clark et al., 2001).

These early Holocene abrupt climate change events were characterized by dry, cool, and windy conditions in the North Atlantic region, although the strength and expression of each event varied geographically (Fleitmann et al., 2008; Hou et al., 2012; Morrill et al., 2013). The 8.2 ka event is unique in the Holocene in terms of its abruptness and magnitude, and is generally considered the most significant climate perturbation of the last 10,000 years (Kobashi et al., 2007). Evidence for the 8.2 ka event, which lasted ~150 years (Thomas et al., 2007) and was characterized by a decrease in mean global annual temperature of 3.3 °C ± 1.1 °C, has been well documented in ice cores (Alley et al., 1997; Kobashi et al., 2007; Rasmussen et al., 2007; Thomas et al., 2007), marine sediments (Keigwin et al., 2005; Daley et al., 2009, Thornalley et al., 2009, 2010) and terrestrial records (Hu et al., 1999; Seppä et al., 2007; Clegg et al., 2011; Gavin et al., 2011; Hou et al., 2012; Moossen et al., 2015; Harning et al., 2018). The 9.3 ka event, which spanned ~110 years according to the INTIMATE event stratigraphy (Blockley et al., 2012), was characterized by a decrease in surface ocean temperature in the North Atlantic and summer temperature on Baffin Island of 1−3 °C (Came et al., 2007; Axford et al., 2009).

Paleo-, observational and modeling studies document that AMOC has multiple stable circulation states and that AMOC has switched between "ON" and "OFF" modes in the past (Rahmstorf, 1995; Clark et al., 2001; Wagner et al., 2013; Ayache et al., 2018) and may do so in the future (Hofmann and Rahmstorf, 2009; Rind et al., 2018). The hypothesis that freshwater input from the collapsing Laurentide Ice Sheet was sufficient to drive the episodic weakening of AMOC during the late Pleistocene and early Holocene is supported by a number of modeling studies (Mikolajewicz et al., 1997; Stouffer et al., 2006; Morrill et al., 2013). The response of AMOC to elevated meltwater flux during the early Holocene was

potentially strong enough to have caused widespread Arctic cooling − despite occurring during a period of high summer insolation and early Holocene warmth (Clark et al., 2001; Briner et al., 2016). For example, the multi-model ensemble mean anomaly of surface mean annual air temperature associated with the 8.2 ka event was estimated to be −0.5 °C in the central Canadian Arctic immediately following the freshwater forcing of the event (Morrill et al., 2013). Although widespread evidence for the 9.3 and 8.2 ka events exist, the magnitude of the associated signal and its spatial imprint reveal that the response of the environment to each forcing was complex and heterogeneous (Fleitmann et al., 2008; Hou et al., 2012; Morrill et al., 2013), complicating our ability to understand early Holocene climate in the North American Arctic (Matero et al., 2017). Characterizing the response of the Arctic climate system to past disruptions of AMOC will provide targets for assessing the sensitivity of the climate system to freshwater forcing and fluctuations in the strength of AMOC that are on-going (Thibodeau et al., 2018; Thornalley et al., 2018). In addition, perturbations in AMOC that are projected to occur in the future (Wagner et al., 2013; Liu et al., 2017; Olson et al., 2018; Rind et al., 2018) due to increased meltwater input from the Greenland Ice Sheet, Canadian Arctic glaciers and northern rivers (albeit weaker) may cause a similar effect on Arctic climate and ecosystems as past fluctuations in AMOC, despite on-going warming (Böning et al., 2016; Liu et al., 2017). Given the potentially disruptive impact of a major change in AMOC, it is imperative to make use of the paleo-record to document the spatial extent of AMOC-related abrupt climate events and gain a better understanding of how fluctuations in AMOC have influenced the Arctic climate system.

Here, we examine the occurrence and magnitude of the 9.3 and 8.2 ka events in the central Canadian Arctic. This region is considered to be one of the most climatically and ecologically sensitive areas to continued anthropogenic climate change (IPCC, 2013) and is expected to be particularly impacted by greenhouse gas induced warming and potentially susceptible to fluctuations in the strength of AMOC (Mahajan et al., 2011). We present quantitative chironomid- and pollen-based air temperature reconstructions for the Holocene from Lake TK2, a small lake located in the central Canadian Arctic, previously shown to be sensitive to early Holocene climate change (Seppä et al., 2003; Paul et al., 2010). Evidence of the sensitivity of the region to the 9.3 and 8.2 ka events is assessed making use of the qualitative and quantitative chironomid and pollen records from Lake TK-2. These records are compared to additional paleolimnological data (e.g. algal data) from the same core to assess the degree of regional landscape and limnic response to the abrupt, short-lived climate events that occurred during the early Holocene. The paleoclimate inferences from Lake TK2 are also compared to existing paleoenvironmental records from areas adjacent to the central Canadian Arctic and further afield to examine the geographic extent of climate and environmental change associated with these events. By providing much-needed quantitative estimates of mean July air temperature (MJAT) we will improve our understanding of the spatial extent, magnitude and seasonality associated with major climatic perturbations such as the 9.3 ka and 8.2 ka events.

1.1. Study site

Lake TK2 (unofficial name; 66.347632°, −104.945688°) is located in the Kitikmeot Region (Nunavut) of the central Canadian Arctic (Fig. 1). The nearest meteorological station to Lake TK2 with a long-term record is located in Cambridge Bay (69.10°, −105.03, 27 m a.s.l.). Mean annual temperature for Cambridge Bay for the period 1971−2000 is −14.4 °C, with a mean summer temperature
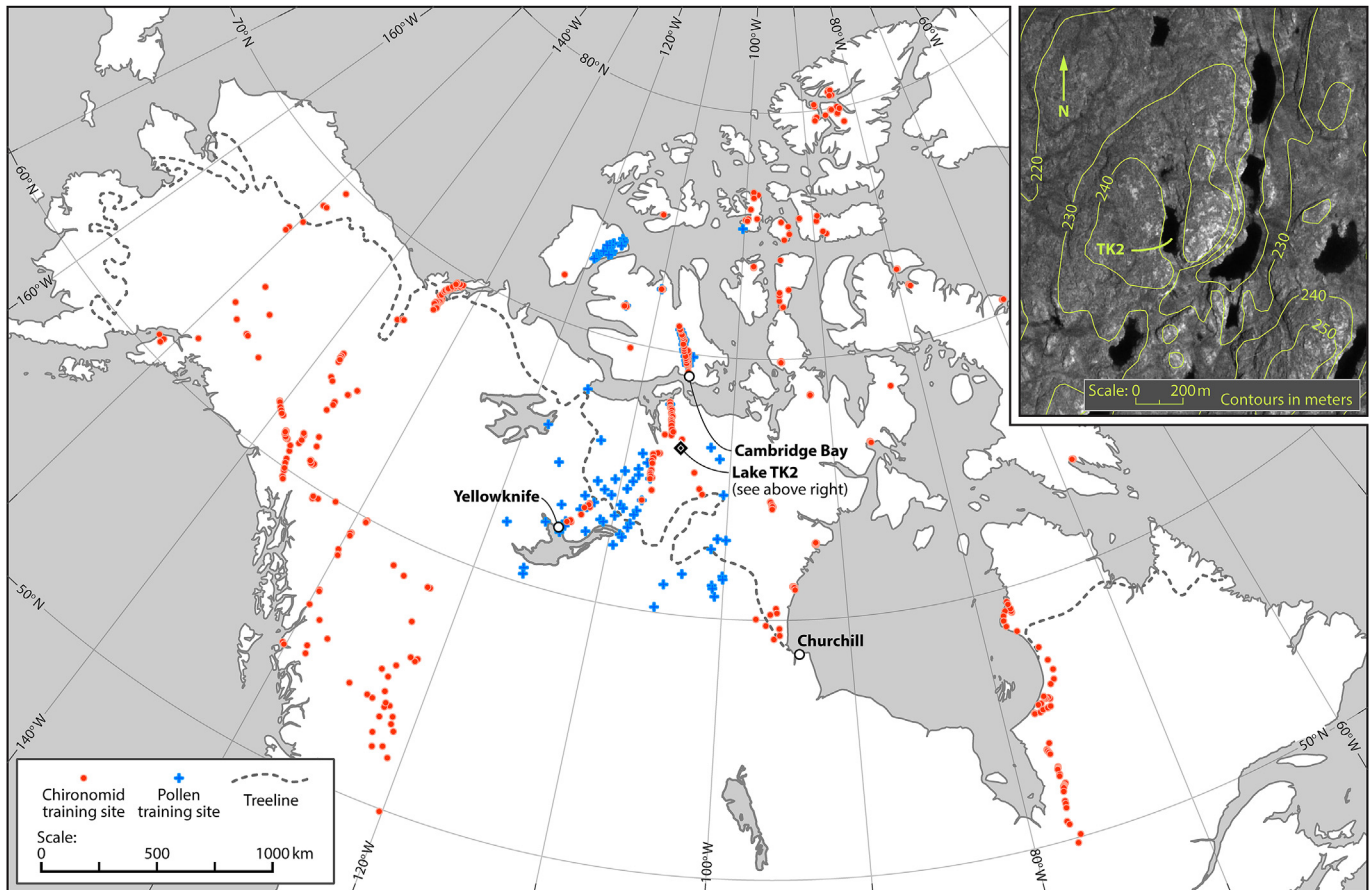
Fig. 1. Location of the lakes incorporated in the North American chironomid (Fortin et al., 2015) and pollen calibration sets and Lake TK2 in the central Canadian Arctic. Inset map depicts topography surrounding Lake TK2 (note wetland to the immediate north of the lake).

(JJA) of 5.7 °C and a mean winter temperature (DJF) of −28.5 °C (Environment Canada, 2002). A gridded climate dataset, based the 1961–1990 Climate Normals, indicates the region surrounding TK2 is characterized by a MJAT of 9.3 °C (New et al., 2002). The lake is located in the low Arctic ecoclimatic region (Ecoregions Working Group, 1989) approximately 200 km north of the forest-tundra ecotone. Lake TK2 is a small (~3 ha), circumneutral (pH = 8.0), ultra-oligotrophic (total phosphorous = 3.1 μgL^{-1}), moderately deep (7.5 m), closed-basin lake underlain by continuous permafrost (Paul et al., 2010). The lake is surrounded by dwarf shrub-lichen, *Betula glandulosa* and *Salix* species; a more detailed description of the vegetation surrounding Lake TK2 is available in Seppä et al. (2003).

2. Material and methods

2.1. Sediment sampling and laboratory analyses

In July 1996, a 198 cm long core was retrieved from the center of Lake TK-2 using a 5 cm diameter modified Livingstone piston sampler (Wright, 1991). The core was kept intact, wrapped in plastic wrap and foil, returned to the laboratory and stored at 4 °C (see Seppä et al. (2003) for further detail). Sixty samples were analyzed for subfossil chironomid remains and pollen. Chironomid head capsules were isolated following standard procedure (Porinchu and MacDonald, 2003). At least 0.5 ml of wet sediment was treated for 15 min in a warm (30 °C) 10% KOH solution and sieved through a 95 μm mesh. Material retained by the sieve was

backwashed into a beaker, poured into a Bogorov counting tray and sorted under a stereomicroscope at 40–50X magnification. Chironomid head capsules were picked using tweezers and permanently mounted in Entellan ®. A minimum of 50 head capsules (Heiri and Lotter, 2001) were identified using a compound light microscope at 400X magnification. Identification of the subfossil chironomids was based on taxonomic guides including Cranston (1982), Oliver and Roussel (1983), Wiederholm (1989), Larocque and Rolland (2006) and Brooks et al. (2007). Loss-on-ignition and pollen analysis were completed and described by Seppä et al. (2003). An estimation of the sediment organic-matter content was calculated by Loss-On-Ignition (LOI) at 550 °C for 4 h (Heiri et al., 2001). Standard methods (Faegri and Iversen, 1989) were used for the preparation of samples for pollen analysis and for pollen counting. A *Lycopodium* tablet was added to each sample to calculate the pollen concentration (Stockmarr, 1971). A minimum of 500 grains were enumerated from most samples to ensure a statistically significant sample size (Maher, 1972). The default pollen sum in Tilia was used as the basal sum for percentage calculations (Grimm, 1990). Diatom data for this study were derived from the fully enumerated diatom record originally published in Paul et al. (2010), but with a focus on several taxa that exhibit noteworthy changes during the intervals of climate change identified in the chironomid and pollen records. Diatom taxa were organized into two groups which displayed similar trends through time including *Karayevia* (*K. laterostrata*, *K. suchlandtii*) and *Nupela* (*Nupela bica-pitata*), as well as several aerophilic diatom taxa (*Navicula schmassmannii, Microcostatus kuelbsii, Diploneis smithii*). Details on

diatom preparation and enumeration methods are described in Paul et al. (2010).

Chronological control of the sediment sequence, as first reported in Seppä et al. (2003), is based on six calibrated AMS radiocarbon dates obtained on bulk sediment for the upper portion of the core and plant macrofossils (twigs) for the remainder of the core (Table 1). The bulk sediment samples were dated at Beta Analytic in Miami, Florida, USA. Pre-treatment with an acid wash did not indicate the presence of $CaCO_3$ in the sediment. Plant macrofossils were dated at IsoTrace Laboratory, Toronto, Canada. The original core chronology presented in Seppä et al. (2003), developed with CALIB 4.3, has been reassessed using CALIB version 7.1 for this study (Stuiver et al., 2019) (Fig. 2). The age-depth model was developed using the BACON package (Blaauw and Christen, 2011).

BACON, which relies on Bayesian statistics, utilizes IntCal13 (Reimer et al., 2013) and the calibration curves associated with each date to derive sediment accumulation rates based on a gamma autoregressive process (Blaauw and Christen, 2011). The BACON program set a gamma distribution (shape = 1.5) for the sedimentation rate with a mean sedimentation rate value determined to be $40 \, yr \, cm^{-1}$. Included in the model was the prior condition that the surface of the core was set to AD 1996 ± 1. The model output includes a goodness-of-fit for each depth with the age reported as calibrated ages (cal yr BP).

2.2. Proxy analyses

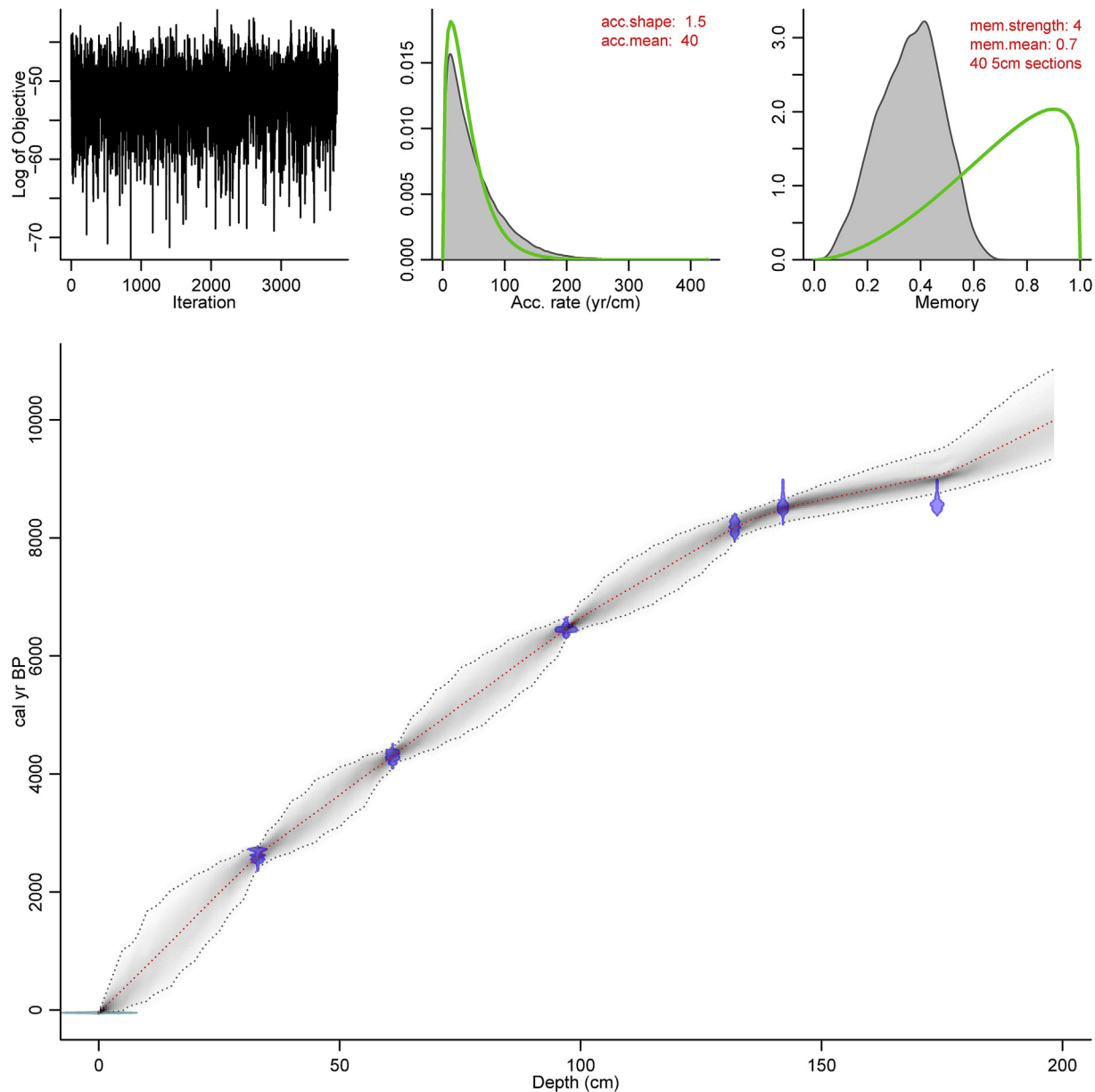The relative abundance of chironomid taxa was plotted

Fig. 2. Age-depth model for the sediment core recovered from Lake TK2 (gray), overlaying the calibrated distributions of individual dates (blue). Gray dots indicate the model's 95% probability intervals, determined using BACON (Blaauw and Christen, 2011). The upper left inset shows the iteration history, the middle inset shows the prior (green line) and posterior (gray area) of the sediment accumulation rate (yr/cm), and the right inset shows the prior (green line) and posterior (gray area) of the memory. (For interpretation of the references to colour in this figure legend, the reader is referred to the Web version of this article.)

stratigraphically using the program C2 (Juggins, 2003). The Hill's N2 diversity index (Hill, 1973) was calculated using Primer 6 (Clarke and Gorley, 2006). Numerical zonation based on an optimal partitioning sum of squares approach was carried out in ZONE (Version 1.2; Juggins, 1992). Detrended Canonical Correspondence Analysis (DCCA), with detrending-by-segments and down-weighting of rare taxa, was implemented to estimate compositional change or turnover (beta diversity) (Birks, 2007).

A two-component weighted averaging partial least squares (WA-PLS) model (ter Braak and Juggins, 1993) was applied to square root transformed chironomid abundance data to reconstruct the MJAT for Lake TK2 (Fortin et al., 2015). The calibration data set used for this reconstruction, which spans the North American Arctic, has a coefficient of determination (r^2_{jack}) of 0.70, a root mean square error of prediction (RMSEP) of 1.93 °C and a maximum bias of 2.22 °C (Fortin et al., 2015). The location of the lakes included in this dataset is shown in Fig. 1. The RMSEP of the chironomid-based inference model is small when considered in relation to the 14.2 °C MJAT range captured by the Fortin et al. (2015) training set, which results in the RMSEP, when expressed as a percentage of the MJAT gradient length, equal to 13.5%. A two-component weighted averaging partial least squares (WA-PLS) model was applied to the square root transformed pollen abundance data to reconstruct MJAT for Lake TK2. The inference model used for the pollen reconstruction, which includes pollen spectra from 108 lakes in the central Canadian Arctic, has a coefficient of determination (r^2_{jack}) of 0.86, a root mean square error of prediction (RMSEP) of 1.41 °C and a maximum bias of 1.90 °C (Fig. 1; Supplementary Material: Tables 1 and 2). The reliability of the quantitative chironomid and pollen-based reconstructions were evaluated by determining: 1) the total percentage of taxa present down-core that are not present in the modern calibration data set; 2) the proportion of rare taxa present in the down-core samples; 3) the squared residual goodness-of-fit (G-O-F) of each chironomid or pollen assemblage to the 1st ordination axis in a canonical correspondence analysis constrained solely by MJAT (Birks, 1998; Engels et al., 2008); and 4) the dissimilarity between each chironomid or pollen sample and its closest modern analogue using a modern analogue technique (MATech) approach based on minimum dissimilarity chord distance (Supplementary Material: Fig. 1). Reconstructions are likely to be most reliable if individual samples are comprised of taxa that are well represented in the calibration set and as a result, have reliable estimates of their optima and tolerances (Birks, 1998). A taxon is classified as rare if it has an effective number of occurrences or Hill's N2 ≤ 5 (Hill, 1973). Taxa with Hill's N2 values > 5 in a training set can be considered well represented and will likely provide reliable estimates of temperature optima (Brooks and Birks, 2001). Samples with a squared residual distance greater than the 90th and 95th percentile of the residual distances of the calibration set samples, were identified as having a 'poor fit' or 'very poor fit' with temperature, respectively (Birks et al., 1990). The 2nd and 5th percentiles of the distribution of dissimilarities, based on the North American Arctic chironomid calibration set (Fortin et al., 2015) or the pollen training set, were used to define the cut-off for 'no close' and 'no good' analogues, respectively (Birks et al., 1990). Sample-specific error estimates were calculated using the program C2 (Juggins, 2003). The existence of climate anomalies in the chironomid- and pollen-based temperature reconstructions was determined using the approach outlined in Morrill and Jacobsen (2005), which makes use of the mean and standard deviation of the proxy values to establish upper and lower bounds of background climate variability for the interval surrounding specific climate events.

3. Results and interpretation

3.1. Core chronology

The revised age-depth model (see Seppä et al. (2003) for original age-depth model) indicates that the basal age of the sediment core recovered from Lake TK2 extends to approximately 10.0 ka, which is 900 years older than the basal age presented in Seppä et al. (2003). The average sediment accumulation rate for the core is 0.02 cm yr^{-1}, with a slight increase in sedimentation rate occurring following 8.2 ka (Fig. 2). The age-depth model and sampling interval result in a multi-centennial sample resolution (200 yr/sample) for sub-fossil chironomid analysis for the entire core with greater resolution available for the intervals centered on 8.2 ka (20 yr/sample) and 9.3 ka (~70 yr/sample). The uncertainty in the age-depth model, as indicated by the 95% confidence bands, is relatively constrained for the entire record (Fig. 2).

3.2. Biostratigraphy

The core has been divided in two statistically distinct zones based on the sub-fossil chironomid stratigraphy (Fig. 3). The pollen data and inferred vegetation conditions are presented and discussed in the context of these zones (Fig. 4).

3.2.1. Zone TK2-1 (~10.0–6.7 ka)

Zone TK2-1, is dominated by *Heterotrissocladius* (~40%), a taxon widely encountered in cold, oligotrophic, Arctic lakes (Olander et al., 1999; Larocque et al., 2006; Porinchu et al., 2009a,b). The base of this zone is characterized by chironomid taxa that are typically associated with recently de-glaciated environments, such as *Microspectra* and *Tanytarsus* (Rolland et al., 2008) and *Stictochironomus,* a profundal taxon, common in cold, deep Arctic lakes (Simola et al., 1996; Walker et al., 1997; Brooks and Birks, 2000; Francis, 2001). The interval between ~9.3 and ~9.1 ka is characterized by increases in *Abiskomyia*, a cold-adapted taxon mainly found in shallow Arctic lakes and flowing waters (Porinchu and Cwynar, 2002; Fortin et al., 2015), and *Paracladius*, a taxon common in cold, Arctic lakes (Fortin et al., 2015). *Abiskomyia* and *Paracladius* have the second and third lowest MJAT optima, respectively, among the seventy-eight chironomid taxa present in the North American chironomid calibration set (Fortin et al., 2015). A decrease in the relative abundance of *Abiskomyia, Paracladius* and *Tanytarsus,* an increase in *Stictochironomus* and the appearance of *Polypedilum* and *Psectrocladius (Monopsectrocladius),* taxa associated with warm, productive lakes (Fortin et al., 2015; Medeiros et al., 2015) occurs between 9.0 and 8.4 ka. *Sergentia* reaches a maximum value of ~35% at ~8.3 ka and subsequently decreases to ~2% at ~8.0 ka. The interval between ~8.2 and ~8.3 ka is characterized by the appearance of a cold-stenotherm, *Hydrobaenus/Oliveridia*, and increases in *Protanypus*, a taxon associated with cold, oligotrophic lakes (Walker and MacDonald, 1995) and *Limnophyes* and *Smittia/Pseudosmittia*, taxa associated with semi-terrestrial and wetland environments (Brooks and Birks, 2004; Heiri, 2004). The upper portion of TK2-1 (~8.0–6.7 ka) is characterized by the disappearance or reduction of cool-water taxa such as *Hydrobaenus/Oliveridia, Paracladius, Microspectra, Sergentia* and *Stictochironomus* and the appearance or increase in thermophilous taxa such as *Microtendipes,* and *Mesocricotopus thienemanni*-type (Walker et al., 1991; Porinchu et al., 2009a,b; Fortin et al., 2015). The Hill's N2 values and DCCA axis 1 scores, which are elevated in TK2-1, indicate that the chironomid assemblage is characterized by greater diversity and ecological turnover in TK2-1 relative to TK2-2. (Fig. 3).
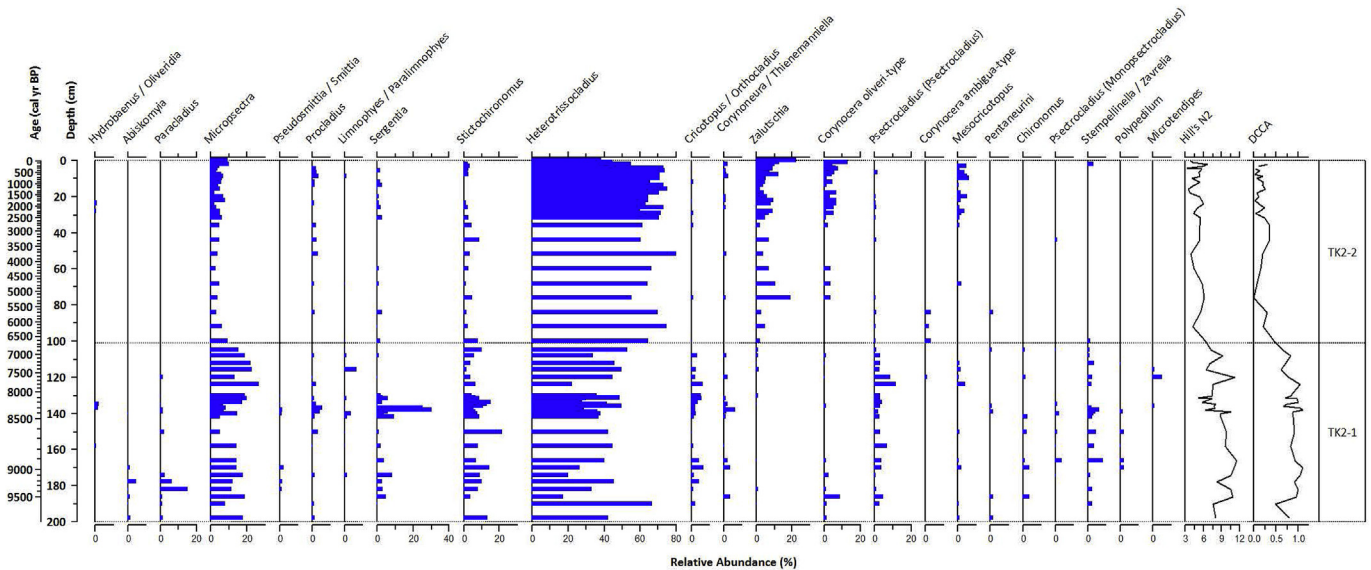
Fig. 3. TK2 chironomid stratigraphy (in relative abundance) based on 58 samples. Zones are based on an optimal partitioning using sum of squares cluster analysis using Zone (Version 1.2; Juggins, 1992). The chironomid taxa are arranged according to their MJAT optima based on Fortin et al. (2015), with *Hydrobaenus/Oliveridia* having the lowest MJAT optimum.

The vegetation community surrounding Lake TK2, which is located approximately 200 km north of modern treeline (Fig. 1), is dominated by shrub tundra, consisting primarily of dwarf birch, for the entire length of the record (Seppä et al., 2003). However, multiple lines of evidence indicate the occurrence of short intervals of instability during the early Holocene. These intervals, centered on 9.3 and 8.2 ka, are characterized by fluctuations in LOI and the relative abundance of *Betula*, Gramineae, Cyperaceae, and *Sphagnum* (Fig. 4 A, B). Decreases in % LOI have been related to decreased lake productivity (Shuman, 2003) and to increased clastic input during periods characterized by increased erosion, which in this region would be expected during colder climates (Lamoureux, 2000). The relative abundance of *Betula* decreases from >50% at the base of the core (~10.0 ka) to 23% at ~ 9.3 ka. Concurrent with the decrease in *Betula* at ~9.3 ka is an increase the relative abundance of Cyperaceae and *Sphagnum* (Seppä et al., 2003) (Fig. 4B). There is also evidence of a distinct disturbance apparent at 8.2 ka, characterized by fluctuations in the relative abundance of *Betula*, Gramineae, Cyperaceae, and *Sphagnum*, and a decrease in LOI (%) (Fig. 4B). Seppä et al. (2003) suggested that the sharp decrease in *Betula* and the increase in the relative abundance of Gramineae, which occurs in conjunction with an increase in Ericaceae, Cyperaceae, *Sphagnum*, and *Vaccinium* at ~ 8.2 ka, reflects a short-lived decrease in the density of dwarf birch cover, which existed prior to the event, to a more open shrub canopy, with sedges and grasses as important components of the vegetation. The vegetation response at ~9.3 ka, which is comparable to the response of vegetation at 8.2 ka, is suggestive of the influence of a similar climate-related forcing at ~9.3 ka. The shift in the composition of the vegetation community at ~9.3 ka, corresponds to a brief, large magnitude increase in the relative abundance of aerophilic diatom taxa (*Navicula schmassmannii*, *Microcostatus kuelbsii*, and *Diploneis smithii*) that are associated with moss (Taylor et al., 2010; Stanek-Tarkowska et al., 2016) (Fig. 4C). Increases in *Karayevia/Nupela* taxa at ~8.2 ka are consistent with a cooler environment as *Karayevia suchlandtii* and *K. laterostrata* have been recorded during cooler periods (Rosén et al., 2000; Bigler and Hall, 2002), whereas *Nupela* taxa are generally considered aerophilic and have been

observed in subaerial epiphytic habitats (Potapova et al., 2003) (Fig. 4C).

3.2.2. Zone TK2-2 (~6.7 ka − present)

The chironomid community in zone TK2-2 is dominated by *Heterotrissocladius*, which increases approximately two-fold to a mean relative abundance of ~65%. The chironomid assemblage at the base of zone TK2-2 is characterized by increases in *Heterotrissocladius*, *Zalutschia*, and *Corynocera ambigua* type and decreases in the relative abundance of *Micropsectra*, *Stictochironomus*, *Protanypus*, *Cricotopus/Orthocladius*, *Psectrocladius (Psectrocladius)*, and *Stempellina/Zavrelia*. The basal portion of TK2-2 is also characterized by reduced diversity and lower ecological turnover. The increase in *Zalutschia* and *Corynocera oliveri*-type at approximately 4.9 ka corresponds to an interval of elevated LOI (%). The chironomid community experiences limited compositional change between ~6.7 and ~2.0 ka, with greater sample-to-sample variability in chironomid community composition characterizing the last ~2 ka. The chironomid assemblage between ~2 ka and the present is characterized by an increasing abundance of *Zalutschia*, *Tanytarsina*, *Corynocera oliveri* type, *Mesocricotopus*, and a decrease in *Heterotrissocladius*. A notable increase in the relative abundance of *Zalutschia* and *Tanytasina*, the reappearance of *Stempellina/Zavrelia*, and a notable decrease in *Heterotrissocladius* occur in the uppermost portion of zone TK2-2, representing the last ~200 years. Also notable is the absence of taxa with low MJAT optima, e.g. *Hydrobaenus/Oliveridia*, *Abiskomyia*, *Paracladius*.

The post-glacial vegetation history developed by Seppä et al. (2003) suggests that climate and vegetation in the vicinity of Lake TK2 remained fairly stable from the mid-Holocene (~6.7 ka) to the present. An observed decrease in *Alnus* (not shown) and increase in Ericaceae at ~ 4.4 ka is inferred to reflect a gradual opening of the *Betula* shrub tundra and possibly decreasing temperature (Seppä et al., 2003). LOI, which increases from below 10% at 7.1 ka to ~20% by 6.5 ka, fluctuates around 15% until ~2 ka. LOI increases during the last two millennia, reaching a core maximum of 40% in the uppermost sediment, which is attributable to an increase in the abundance of aquatic moss in recent centuries (Seppä et al., 2003).
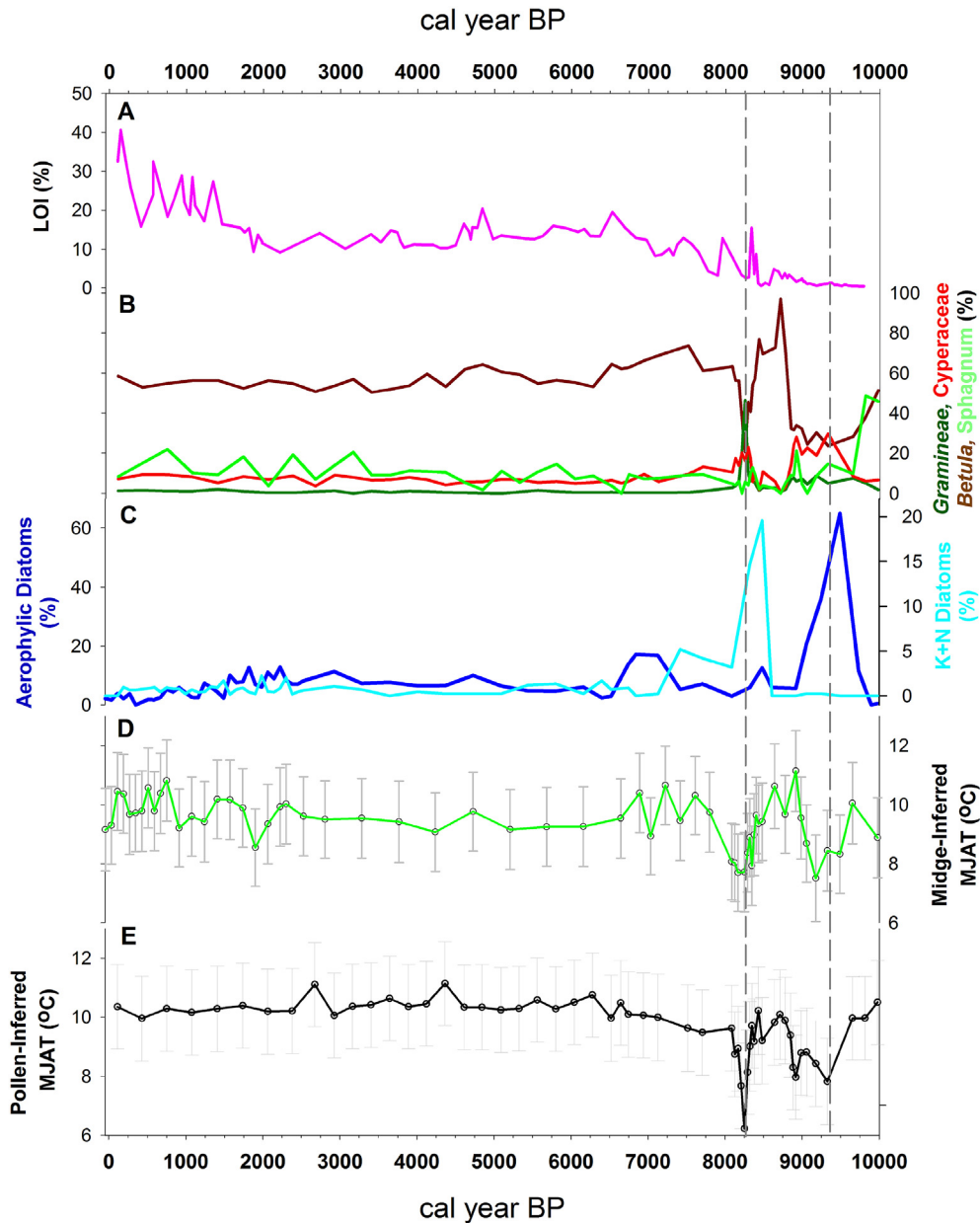
Fig. 4. (A) Loss-on-Ignition (%). (B) Relative abundance (%) of *Betula*, Cyperaceae, Gramineae and *Sphagnum* (10X exaggeration) pollen. (C) Aerophilic diatom taxa (*Navicula schmassmannii, Microcostatus kuelbsii, Diploneis smithii*) and *Karayevia* and *Nupela* (Paul et al., 2010). (D) Chironomid-inferred mean July air temperature reconstructions with sample-specific error bars for Lake TK2. (E) Pollen-inferred July temperature reconstruction with sample-specific error bars for Lake TK2. Dashed lines depict the 8.2 and 9.3 ka events.

3.3. Chironomid and pollen-based temperature reconstructions

The chironomid- and pollen-inferred temperature re-constructions and the associated sample specific error estimates are presented in Fig. 4D and E. Sample-specific error estimates for the chironomid- and pollen-inferred MJAT ranged between 1.9 °C and 2.0 °C and 1.4 °C and 1.7 °C, respectively. The reliability of the quantitative chironomid- and pollen-based temperature recon-struction was evaluated using a number of approaches (Supplementary Material: Fig. 1).

An assessment of the total percentage of taxa present down-core that do not appear in the modern calibration data set indi-cated that the subfossil chironomid taxa present in TK2 are well-

represented and characterized in the northern North American chironomid calibration set with all thirty chironomid taxa identi-fied in TK2 present in the northern North American training set (Fortin et al., 2015). The optima and tolerances of these thirty taxa are also well-defined by the North American chironomid calibra-tion set with the Hill's N2 values for the taxa present in the TK2 record varying between 18 and 433 in the modern training set. Analyses of the reliability of the quantitative chironomid-based temperature reconstruction using modern analogue technique (MATech) and goodness of fit (G-O-F) approaches suggest that the chironomid-based reconstruction can be considered robust (Supplementary Material: Fig. 1). The G-O-F analysis indicates that the downcore sample scores for the subfossil chironomids, which

fluctuate well below the 90th percentile cut-levels, with the exception of one sample at ~470 cal yr BP, have a good fit to temperature and can be considered very reliable (Engels et al., 2008). The MATech analysis indicates that the subfossil assemblages have close analogues in the modern training set (Fortin et al., 2015) with the exception of samples at ~ 8.3, 8.6, and 9.0 ka, all of which can be considered as having good analogues in the modern training set (Birks et al., 1990). The reliability measures indicate that the chironomid-inferred estimates for July air temperature at ~8.2 and 9.3 ka can be considered very reliable.

The thirty-six pollen taxa identified in TK2 are present in the regional pollen calibration (Supplementary Material: Table 2). The proportion of rare pollen taxa present in the down-core samples is low as reflected by the Hill's N2 diversity index values, which ranged between 1.3 and 77, with only three pollen taxa present in the TK2 pollen stratigraphy (*Corylus, Rubus, Rumex*) having Hill's N2 values less than three in the training set (not shown). *Corylus*, which is not a part of the regional flora, was likely transported long-distance from further south; *Corylus* pollen has been recorded in ice cores on Devon Island (McAndrews, 1984). *Rubus* and *Rumex* were present in only three downcore samples and did not exceed >0.20% of the total pollen spectra in any sample. The G-O-F analysis indicates that the downcore sample scores for the pollen assemblages fluctuate below the 95th percentile cut-levels, with the exception of five samples: at ~8.3—8.4 ka, 8.7 and 9.0 cal yr BP. The MATech analysis indicates that the pollen assemblages have close analogues in the modern training set for the interval 8.2 ka to the present; the early Holocene portion of the core (9.7—8.2 ka) lack good analogues in the modern pollen training set (Birks et al., 1990). An assessment of the reliability of the quantitative pollen-based temperature reconstruction using modern analogue technique (MATech) and Goodness-of-Fit (G-O-F) approaches suggest that the mid-to late-Holocene portion of the TK2 pollen-based reconstruction can be considered reliable; however, the early Holocene portion of the pollen reconstruction cannot be considered robust (Supplementary Material: Fig. 1).

The chironomid-and pollen-based reconstructions indicate that the mean July air temperature for the last ~10.0 ka was 9.4 °C and 9.7 °C, respectively. The range of reconstructed temperatures captured by variations in the chironomid community and pollen spectra at TK2 was 3.6 °C (11.1—7.5 °C) and 4.9 °C (11.1—6.2 °C), respectively. Notable deviations from the Holocene average, apparent in both the pollen and chironomid-based July temperature reconstructions, occur at ~9.3 ka and 8.2 ka. Although the pollen and chironomid-based estimates for the 9.3 ka and 8.2 ka excursions are comparable, the temperature estimates reported for the early Holocene portion of the core focus on the more statistically reliable chironomid-based reconstruction. The chironomid-based temperature estimate is ~1.4 °C (8.0 °C) and ~1.7 °C (7.7 °C) lower than the long-term Holocene average, at 9.3 and 8.2 ka, respectively. Following the climate cooling at ~8.2 ka, the chironomid-inferred July air temperatures increase to a mid-Holocene maximum of ~10.7 °C at ~7.2 ka (Fig. 4D). The chironomid-inferred temperatures remain relatively stable, fluctuating around ~9.7 °C, for much of the mid-Holocene, with notable sample-to-sample variability in the chironomid-inferred temperatures characterizing the late Holocene. The pollen-inferred reconstruction shows less variation than the chironomid-inferred reconstruction with the pollen-inferred MJAT fluctuating around a fairly stable mean of 10.4 °C during the mid-to late Holocene with a peak of 11.1 °C occurring at ~4.4 ka. Application of the climate anomaly test, outlined in Morrill and Jacobsen (2005), identified that existence of statistically significant temperature anomalies between ~ 8.3 and 8.15 ka in the chironomid-based reconstruction (Supplemental Material: Table 3).

4. Discussion

Multi-proxy analysis of lake sediment archives has improved our understanding of climate and environmental variability in the Arctic, which is vital as instrumental records in this region are typically limited to the last 50—70 years (Kaufman et al., 2004, 2016; Gajewski, 2015; Briner et al., 2016). For example, numerous studies have documented the occurrence of dramatic alterations in high latitude aquatic ecosystem structure and composition during the late 20th and early 21st centuries in response to elevated temperatures (Smol et al., 2005; Smol and Douglas, 2007; Rühland et al., 2008, 2015). Observations of the effects of anthropogenic climate change on the contemporaneous Arctic environment has highlighted the need for lengthier reconstructions of past climate variability and associated impacts on terrestrial and aquatic ecosystems (Hu et al., 2015; Schuur et al., 2015; Notz and Stroeve, 2016; Hobbie et al., 2017; Pecl et al., 2017). The two most abrupt, prominent climate events of the Holocene, as defined by excursions in the $\delta^{18}O$ in Greenland ice cores, occurred at 8.2 ka and 9.3 ka (Alley et al., 1997; Kobashi et al., 2007; Rasmussen et al., 2007; Thomas et al., 2007). Yet, these events remain poorly characterized in the North American Arctic, with the number of quantitative estimates of the temperature change at 8.2 ka and 9.3 ka relatively limited (Fleitmann et al., 2008; Morrill et al., 2013). Although an increasing number of paleolimnological studies have documented the response of Arctic ecosystems to low frequency climate change during the Holocene, few records from the central Canadian Arctic have documented the response of climate and landscape to the abrupt centennial-scale climate perturbations that occurred during the early Holocene (Seppä et al., 2003; Axford et al., 2009; Paul et al., 2010). To our knowledge the chironomid-based temperature record developed for TK2 is the first such quantitative reconstruction in the central Canadian Arctic that captures both of these widespread, early Holocene climate anomalies.

Recent reviews have highlighted the critical assumptions underlying quantitative paleolimnology (Birks et al., 2010), cautioned against the indiscriminate application of quantitative transfer functions (Juggins, 2013; Huntley, 2012), and discussed the confounding effects of correlated environmental variables on quantitative reconstructions (Velle et al., 2010, 2012). Notably these reviews all highlight the need for a sound understanding of the (paleo)ecology of the organism and the requirement that a strong causal relationship exists between the variable of interest and the biological proxy (Juggins and Birks, 2012). The influence of air and water temperature on the developmental stages of chironomids and the ecological response of midges to temperature has been well documented (Eggermont and Heiri, 2012). The strong direct relationship between chironomids and summer temperature, which has been demonstrated to drive the distributional changes of chironomids at the landscape scale (Walker and Cwynar, 2006; Brooks et al., 2012; Barber et al., 2013), substantiates the use of midges as proxies for Holocene temperature (Brooks et al., 2012). The close correspondence and agreement between the independent terrestrial (pollen) and aquatic (chironomid) proxy-based reconstructions and the response of the diatom community at 9.3 and 8.2 ka further supports the use of the chironomids in deriving estimates of MJAT and emphasizes the value of implementing multiproxy approaches to reconstruct past climates and environments.

Lake TK2 was characterized by two major phases during the Holocene. The first phase, spanning the interval between ~10.0 ka and ~6.7 ka, was characterized by notable chironomid compositional turnover and fluctuations in Gramineae, *Betula* and Cyperaceae pollen. The chironomid assemblages preserved in Lake TK2 clearly reveal the presence of a cold-adapted community through

the entire Holocene; however, the appearance of taxa typically associated with more productive ecosystems at the base of TK2-1 suggest that the trajectory of the lake moved rapidly from an early post-glacial environment to a more productive aquatic system during the early Holocene. This inference is corroborated by the trend of increasing %LOI values between ~10.0 ka and ~6.7 ka. This early phase is punctuated by intervals characterized by increases in cold-adapted chironomid taxa, such as *Hydrobaenus/Oliveridia*, *Abiskomyia*, and *Sergentia*, and taxa associated with semi-terrestrial and wetland habitats, such as *Limnophyes/Paralimnophyes*, and *Smittia/Pseudosmittia*. The presence of *Smittia/Pseudosmittia* and *Limnophyes/Paralimnophyes*, together with an increase in the relative abundance of *Sphagnum*, is inferred to reflect the occurrence of wetter conditions at 9.3 ka and 8.2 ka, respectively. This inference is also supported by abrupt, short-lived increases in diatom taxa including aerophilic epiphytic diatom species, such as *Navicula schmassmannii*, *Microcostatus kuelbsii*, and *Diploneis smithii* at ~9.3 ka, which suggests a corresponding increase in littoral habitat that includes greater availability of epiphytic habitats, including mosses. This is followed by an increase in *Karayevia/Nupela* diatom taxa at 8.2 ka, which likely reflect increased effective moisture and cold conditions (Rosén et al., 2000; Potapova et al., 2003). Although somewhat speculative, an increase in littoral environments would occur at TK2 with wetter conditions. Wetter conditions during these two cold events would have resulted in rising lake levels, which would have led to flooding of a wetland area north of TK2 (Fig. 2) and resulted in an expansion of semi-terrestrial habitats. This would have favored an increase in aerophilic diatom and chironomid taxa and *Sphagnum*. The brief increase in these biotic proxies corresponds well with the timing of pollen and chironomid-inferred MJAT temperature minima at 9.3 and 8.2 ka (Fig. 4). Further, this inference of cold-wet synoptic climate conditions, characterized by depressed temperature and elevated humidity is supported by the existence of a negative relationship between temperature and precipitation in the central Canadian Arctic during cold intervals in recent centuries (Lamoureux, 2000).

The second phase, TK2-2, spans the interval from ~6.7 ka to the present and corresponds to the stabilization of the chironomid community, suggested by lower faunal turnover, as indicated by the DCCA scores, reflecting reduced climate and environmental variability, until ~2.0 ka, at which point sample-to-sample variability in the chironomid assemblages increases. The increase in sample-to-sample variability in the midge assemblages at Lake TK2 during the late Holocene corresponds to increasing sediment organic content (as estimated by LOI) and elevated chironomid-inferred MJAT (2 ka average MJAT = 9.80 °C). Existing high-resolution (multi-decadal) chironomid stratigraphies from the central Canadian Arctic spanning the last two millennia are characterized by notable variability in composition particularly after ~1500 AD (MacDonald et al., 2009; Porinchu et al., 2009b). The elevated temperature evidenced at Lake TK2 during recent centuries broadly fits the pattern of warming observed in temperature sensitive biogenic silica records from the treeline zone to south (MacDonald et al., 2009) and sites located further north in the northern Canadian Arctic mainland (Peros and Gajewski, 2009) and the Canadian Arctic Archipelago (Finkelstein and Gajewski, 2007; Porinchu et al., 2009b). The cooling apparent in the samples representing the 20th century at Lake TK2 may reflect the development or strengthening of lake stratification, a pattern that has been observed elsewhere in the central Canadian Arctic in recent decades (MacDonald et al., 2009; Porinchu et al., 2009b).

The climate and associated environmental instability observed at Lake TK2 during the early Holocene resulted from the influence of the continued retreat of the Laurentide Ice Sheet on atmospheric circulation in the sub-Arctic and Arctic (Clarke et al., 2003, 2009). The chironomid-inferred MJAT reconstruction indicates that the early portion of the Holocene, between 8.9 and 8.6 ka, was the warmest sustained interval of the last ~10 ka. The average chironomid-inferred MJAT for this interval (10.2 °C) is ~0.8 °C higher than the Holocene chironomid-inferred average MJAT. This corresponds well with ice core and pollen-based reconstructions that suggest maximum July temperatures occurred in the central and high Canadian Arctic prior to 8.0 ka and is consistent with orbital forcing (Vinther et al., 2009; Gajewski, 2015; Briner et al., 2016; Lecavalier et al., 2017). The onset of chironomid-inferred cooling during the mid-Holocene at Lake TK2, which occurs at ~6.7 ka when MJAT drops to 9.5 °C from 10.4 °C at 6.9 ka, closely tracks the onset of chironomid-inferred cooling at Lake KR02, Victoria Island (Briner et al., 2016). The minima in chironomid-inferred MJAT at Lake TK2, which occurs between 1.8 and 1.5 ka, broadly corresponds to a chironomid-based reconstruction from Carleton Lake, NWT (Upiter et al., 2014), which indicates the coldest inferred temperatures over the last 6,000 years occurred at approximately 1.6 ka, and the timing of depressed Holocene temperatures in the central Canadian Arctic identified in a regional synthesis for the central Canadian Arctic (Gajewski, 2015).

The chironomid-based temperature reconstruction from TK2 indicates that early peak Holocene warmth in the central Canadian Arctic was interrupted by two rapid, centennial-scale cooling events at 9.3 ka and 8.2 ka. The magnitude of chironomid-inferred cooling associated with these events, which was 1.4 °C and 1.7 °C (relative to the long-term Holocene temperature), compare favorably with the pollen-based estimates (1.6 °C and 2.0 °C) from the same core, although the latter cannot be considered statistically robust. Recent syntheses reveal a paucity of comparative records in the central Canadian Arctic that provide quantitative estimates of thermal conditions explicitly associated with the 8.2 ka and 9.3 ka events (Fleitmann et al., 2008; Morrill et al., 2013; Gajewski, 2015; Briner et al., 2016). A quantitative reconstruction of early Holocene thermal conditions in the eastern Canadian Arctic does provide evidence that early Holocene warmth was interrupted by cold reversals at ~9.3—9.2 ka and ~8.5 ka (Axford et al., 2009). The depression of mean July air temperature at Lake CF8 on Baffin Island was ~0.7 °C and 1.5 °C (relative to the long-term Holocene average) at ~ 9.2 ka and 8.5 ka, respectively (Axford et al., 2009). A composite record of quantitative chironomid-based temperature reconstructions from southern British Columbia reveals a similar pattern: elevated mean July air temperature during the early Holocene interrupted by two short-lived events of depressed MJAT at ~9.3 ka and 8.2 ka (Gavin et al., 2011). A chironomid-based composite MJAT reconstruction, derived from sites located in central and south-central Alaska, also suggests that the interval spanning the 8.2 ka event was characterized by below-modern temperature (Clegg et al., 2011). Well-constrained records of outlet-glacier change in western Greenland indicates that glacier retreat during the early Holocene was punctuated by two notable re-advances at ~9.3 ka and 8.2 ka (Young et al., 2011, 2013). These records provide further, independent support of the occurrence of short-lived episodes of climatic deterioration in the sub-Arctic and Arctic of North America during these intervals. In addition, ice cores and marine sediment records suggest that surface temperatures were depressed by 2—6 °C in central Greenland (Masson-Delmotte et al., 2005; Rohling and Pälike, 2005; Kobashi et al., 2007) and 1—3 °C in the North Atlantic and Europe (Came et al., 2007; Fleitmann et al., 2008; Morrill et al., 2013) during these abrupt early Holocene climate events.

Variations in our multi-decadal-scale chironomid- and pollen MJAT estimates in the central Canadian Arctic at 9.3 and 8.2 ka
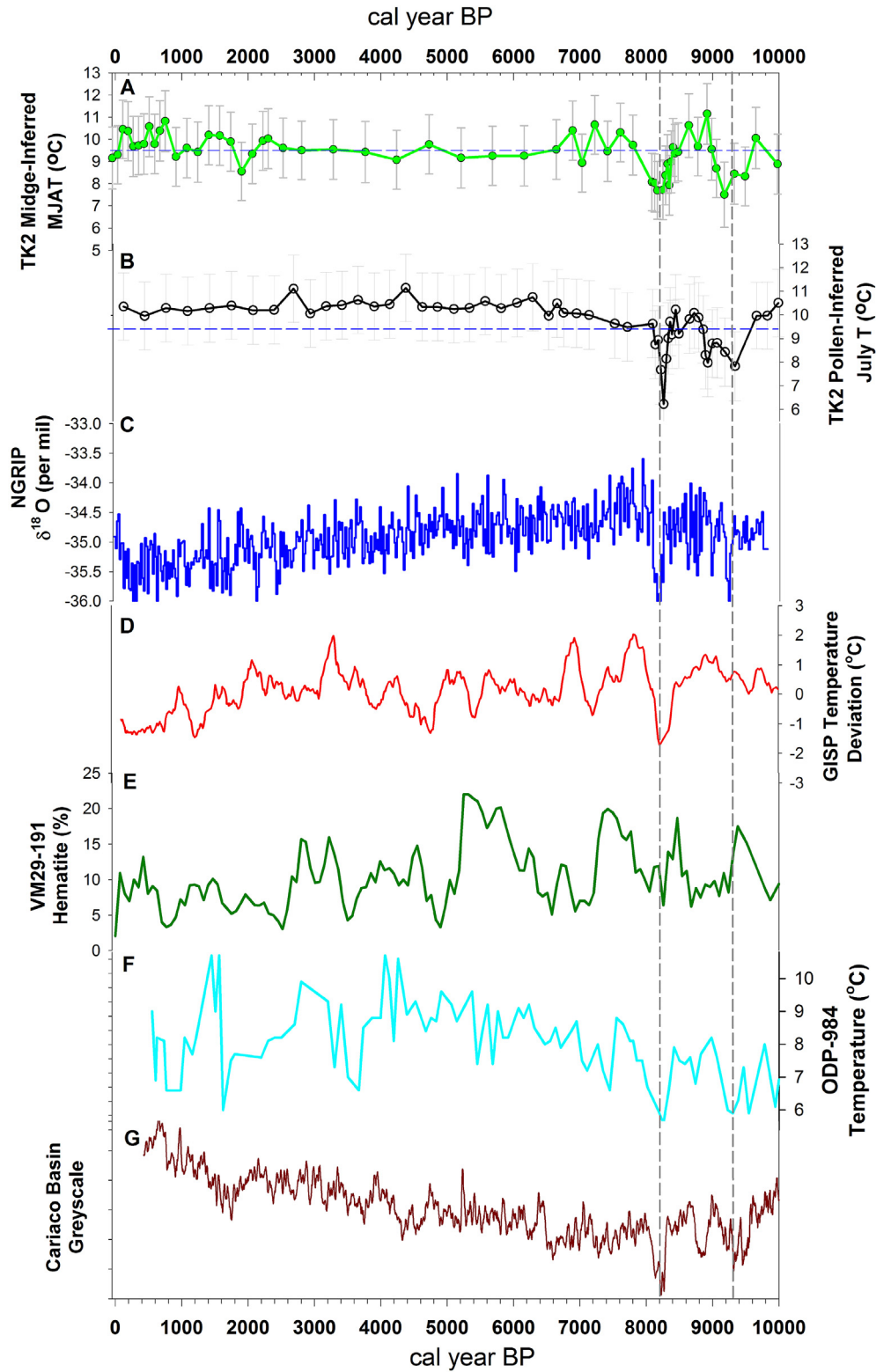
Fig. 5. (A) Chironomid-inferred mean July air temperature reconstructions with sample-specific error bars for Lake TK2. (B) Pollen-inferred July temperature reconstruction with sample-specific error bars for Lake TK2. (C) $\delta^{18}O$ from NGRIP (North Greenland Ice Core Project Members, 2004). (D) Temperature deviations estimated from $\delta^{18}O$ variations in GISP2 (Alley, 2004). (E) % hematite stained grains from core VM-29-191 (Bond et al., 2001). (F) Average Mg/Ca-derived temperature estimates based on planktonic foraminifera from ODP-964 (Came et al., 2007). (G) Gray scale from Cariaco Basin (Hughen et al., 2000). Dashed lines depict the 8.2 and 9.3 ka events.

coincide with AMOC related oscillations evidenced in the North Atlantic and elsewhere in the Northern Hemisphere (Hou et al., 2012). There is compelling evidence for the existence of a relationship between repeated episodes of AMOC weakening, likely associated with multiple meltwater pulses into the North Atlantic during the early Holocene, and climatic oscillations, including the 8.2 ka event (Hoffman et al., 2012) and 9.3 ka event (Fleitmann et al., 2008; Yu et al., 2010; Hou et al., 2012). Existing proxy records (Barber et al., 1999; Ellison et al., 2006; Carlson et al., 2009; Törnqvist and Hijma, 2012; Estrella-Martínez et al., 2019) and climate model experiments (LeGrande et al., 2006; Wiersma and Renssen, 2006; Clarke et al., 2009; Wiersma et al., 2011) support the hypothesis that the 8.2 event was a response to large-scale ocean and atmosphere forcing potentially related to the final collapse of the Laurentide Ice Sheet (Matero et al., 2017) and/or the drainage of Glacial Lake Agassiz, resulting in suppressed AMOC (Thomas et al., 2007; Hoffman et al., 2012). However, there remain uncertainties regarding the source, timing and pathway of the meltwater pulse (Teller et al., 2002; Gregoire et al., 2012) and the relative influence of various climate forcings (Rohling and Pälike, 2005). The spatial pattern and the magnitude of cooling associated with 9.3 ka event is similar to the perturbation at 8.2 ka with evidence for this event also strongly expressed in the North Atlantic, Greenland, eastern and western North America, central Europe and east Asia (Fleitmann et al., 2008; Gavin et al., 2011; Hou et al., 2012; Briner et al., 2016; Kaufman et al., 2016). To date, no known model experiments have assessed climate model skill at simulating the response of the climate system to North Atlantic freshwater forcing coeval with 9.3 ka.

Modeling studies suggest that a large negative salinity anomaly in the North Atlantic weakened AMOC sufficiently to cause dramatic cooling across the circum- North Atlantic and further afield during the early Holocene (Morrill et al., 2013). The strong correspondence in the timing and duration of the events as recorded in speleothems in east Asia (Dykoski et al., 2005; Wang et al., 2005; Liu et al., 2013), lake records in temperate, subarctic, and Arctic North America and Europe (von Grafenstein et al., 1999; Seppä et al., 2009; Clegg et al., 2011; Gavin et al., 2011; Hou et al., 2012; *this study*), ice cores and moraines in Greenland (Alley et al., 1997; Young et al., 2013) and marine sediment records from the North Atlantic and tropical Atlantic (Hughen et al., 2000; Ellison et al., 2006; Came et al., 2007; Thornalley et al., 2009, 2010; Lewis et al., 2012) provide evidence for the strong coupling of North Atlantic SSTs (Came et al., 2007) and AMOC (Hughen et al., 2000; Bond et al., 2001; Ayache et al., 2018) with hemispheric climate conditions (North Greenland Ice Core Project, 2004) (Fig. 5). For example, these proxy-based studies document a southward shift of the ITCZ in both the Atlantic and Pacific oceans (Hughen et al., 2000; Cheng et al., 2009; Voarintsoa et al., 2019) and weaker Asian (Liu et al., 2013; Zhang et al., 2018) and Indian Summer Monsoons (Dixit et al., 2014) during early Holocene cold intervals. However, the majority of climate models underestimate the magnitude and duration of the cooling associated with these abrupt, early Holocene climate events. Coupled-ocean atmosphere and Earth systems models simulating the climate perturbation at 8.2 ka resolve an event that lasts only a few decades and a reduction in temperature that is notably less than the proxy-based estimates (Morrill et al., 2013). The magnitude of the simulated cooling associated with the 8.2 ka event (Clarke et al., 2009; Morrill et al., 2013) is approximately 33—50% of the proxy-based inferences (von Grafenstein et al., 1999; Kobashi et al., 2007; Seppä et al., 2009; *this study*).

This research provides a benchmark which can be used to refine and further test of the veracity of coupled-ocean atmosphere

climate models simulating the response of the climate system to variations in AMOC. Addressing the inconsistencies between the modeling studies and proxy inferences is critical, as the response of the central Canadian Arctic to the projected freshening of the North Atlantic in coming decades is relevant to modeling future climate change in the Arctic (Lamoureux et al., 2006). As evident here, the sensitivity of central Canadian Arctic limnic ecosystems and tundra vegetation to early Holocene variations in AMOC suggests that the aquatic and terrestrial environment of the region will likely be sensitive to future changes in the AMOC. This is particularly important because climate models suggest that the observed decrease in the strength of the AMOC that is currently occurring due to increased meltwater flux from Greenland and the Canadian Arctic will continue in response to anthropogenic forcing (Rahmstorf et al., 2015; Caesar et al., 2018; Smeed et al., 2018). Most climate models predict that AMOC will slow in coming decades but not undergo a complete shutdown, although the degree of change is not certain (Schmittner et al., 2005). However, studies published within the last decade suggest that the existing inter-model consensus, which may be an artifact resulting from a common model bias favoring a stable AMOC (Hofmann and Rahmstorf, 2009; Hawkins et al., 2011; Liu et al., 2017), may underestimate the magnitude of cooling associated with the projected freshening of the North Atlantic in coming centuries (Hansen et al., 2016; Liu et al., 2017).

5. Conclusions

The chironomid- and pollen-based reconstructions from Lake TK2 provide evidence that the early Holocene in the central Canadian Arctic was characterized by notable fluctuations in mean July air temperature and provides the first quantitative estimate of the magnitude of this temperature change in mean July air temperature for the ~9.3 and 8.2 ka events in this region. The correspondence between the independent terrestrial (pollen) and aquatic (chironomid) proxy-based reconstructions at 9.3 and 8.2 ka highlights the utility of multi-proxy approaches to reconstructing past climate and environment and strongly supports the use of chironomids in deriving quantitative estimates of MJAT. The chironomid-based estimates indicate that MJAT decreased: 1) 1.4 °C at ~9.3 ka; and 2) 1.7 °C between at 8.2 ka, relative to the long-term Holocene average. Chironomid and diatom evidence also point to wetter conditions and an expansion of moss habitats during these cold periods. The timing of these events in the central Canadian Arctic corresponds well with paleoclimate records from the adjacent region and far afield, strongly supporting the role of atmospheric and oceanic teleconnections in transmitting the signal associated with these early Holocene climate oscillations with enough magnitude to produce rapid shifts in aquatic and terrestrial ecosystems. Further characterizing the magnitude and spatial extent of these hemisphere-scale, abrupt climate events is important in anticipating the potential climatic and environmental impacts of changes in systems such as the AMOC, which will be altered in coming decades by anthropogenic climate change.

Appendix A. Supplementary data

Supplementary data to this article can be found online at https://doi.org/10.1016/j.quascirev.2019.07.024.

References

Alley, R.B., Mayewski, P.A., Sowers, T., Stuiver, M., Taylor, K.C., Clark, P.U., 1997. Holocene climatic instability: a prominent, widespread event 8200 yr ago. Geology 25 (6), 483–486.

Axford, Y., Briner, J.P., Cooke, C.A., Francis, D.R., Michelutti, N., Miller, G.H., Smol, J.P., Thomas, E.K., Wilson, C.R., Wolfe, A.P., 2009. Recent changes in a remote Arctic lake are unique within the past 200,000 years. Proc. Natl. Acad. Sci. 106 (44), 18443–18446.

Ayache, M., Swingedouw, D., Mary, Y., Eynaud, F., Colin, C., 2018. Multi-centennial variability of the AMOC over the Holocene: a new reconstruction based on multiple proxy-derived SST records. Glob. Planet. Change. 170, 172–189.

Barber, D.C., Dyke, A., Hillaire-Marcel, C., Jennings, A.E., Andrews, J.T., Kerwin, M.W., Bilodeau, G., McNeely, R., Southon, J., Morehead, M.D., Gagnon, J.M., 1999. Forcing of the cold event of 8,200 years ago by catastrophic drainage of Laurentide lakes. Nature 400 (6742), 344–348.

Barber, A., Brown, A., Langdon, P., Hughes, P., 2013. Comparing and cross-validating lake and bog palaeoclimatic records: a review and a new 5,000 year chironomid-inferred temperature record from northern England. J. Paleolimnol. 49 (3), 497–512.

Berger, A., Loutre, M.F., 1991. Insolation values for the climate of the last 10 million years. Quat. Sci. Rev. 10 (4), 297–317.

Bigler, C., Hall, R.I., 2002. Diatoms as indicators of climatic and limnological change in Swedish Lapland: a 100-lake calibration set and its validation for paleoecological reconstructions. J. Paleolimnol. 27 (1), 97–115.

Birks, H.J.B., 1998. DG Frey and ES deevey review 1: numerical tools in palaeolimnology—progress, potentialities, and problems. J. Paleolimnol. 20 (4), 307–332.

Birks, H.J.B., 2007. Estimating the amount of compositional change in late-Quaternary pollen-stratigraphical data. Veg. Hist. Archaeobotany 16 (2–3), 197–202.

Birks, H.J.B., Line, J.M., Juggins, S., Stevenson, A.C., Ter Braak, C.J.F., 1990. Diatoms and pH reconstruction. Philos. Trans. R. Soc. Lond. B Biol. Sci. 327 (1240), 263–278.

Birks, H.J.B., Heiri, O., Seppä, H., Bjune, A.E., 2010. Strengths and weaknesses of quantitative climate reconstructions based on Late-Quaternary. Open Ecol. J. 3 (1).

Blaauw, M., Christen, J.A., 2011. Flexible paleoclimate age-depth models using an autoregressive gamma process. Bayesian Anal. 6 (3), 457–474.

Blockley, S.P., Lane, C.S., Hardiman, M., Rasmussen, S.O., Seierstad, I.K., Steffensen, J.P., Svensson, A., Lotter, A.F., Turney, C.S., Ramsey, C.B., Intimate Members, 2012. Synchronisation of palaeoenvironmental records over the last 60,000 years, and an extended INTIMATE event stratigraphy to 48,000 b2k. Quat. Sci. Rev. 36, 2–10.

Bond, G., Kromer, B., Beer, J., Muscheler, R., Evans, M.N., Showers, W., Hoffmann, S., Lotti-Bond, R., Hajdas, I., Bonani, G., 2001. Persistent solar influence on North Atlantic climate during the Holocene. Science 294 (5549), 2130–2136.

Böning, C.W., Behrens, E., Biastoch, A., Getzlaff, K., Bamber, J.L., 2016. Emerging impact of Greenland meltwater on deepwater formation in the North Atlantic Ocean. Nat. Geosci. 9 (7), 523.

Briner, J.P., McKay, N.P., Axford, Y., Bennike, O., Bradley, R.S., de Vernal, A., Fisher, D., Francus, P., Fréchette, B., Gajewski, K., Jennings, A., 2016. Holocene climate change in Arctic Canada and Greenland. Quat. Sci. Rev. 147, 340–364.

Brooks, S.J., Birks, H.J.B., 2000. Chironomid-inferred late-glacial and early-Holocene mean July air temperatures for Kråkenes Lake, western Norway. J. Paleolimnol. 23 (1), 77–89.

Brooks, S.J., Birks, H.J.B., 2001. Chironomid-inferred air temperatures from Late-glacial and Holocene sites in north-west Europe: progress and problems. Quat. Sci. Rev. 20 (16), 1723–1741.

Brooks, S.J., Birks, H.J.B., 2004. The dynamics of Chironomidae (Insecta: Diptera) assemblages in response to environmental change during the past 700 years on Svalbard. J. Paleolimnol. 31 (4), 483–498.

Brooks, S.J., Langdon, P.G., Heiri, O., 2007. Using and Identifying Chironomid Larvae in Palaeoecology, QRA Technical Guide No 10. Quaternary Research Association, London.

Brooks, S.J., Axford, Y., Heiri, O., Langdon, P.G., Larocque-Tobler, I., 2012. Chironomids can be reliable proxies for Holocene temperatures. A comment on Velle et al.(2010). Holocene 22 (12), 1495–1500.

Buckley, M.W., Marshall, J., 2016. Observations, inferences, and mechanisms of the atlantic meridional overturning circulation: a review. Rev. Geophys. 54 (1), 5–63.

Caesar, L., Rahmstorf, S., Robinson, A., Feulner, G., Saba, V., 2018. Observed fingerprint of a weakening Atlantic Ocean overturning circulation. Nature 556 (7700), 191.

Came, R.E., Oppo, D.W., McManus, J.F., 2007. Amplitude and timing of temperature and salinity variability in the subpolar North Atlantic over the past 10 ky. Geology 35 (4), 315–318.

Carlson, A.E., Anslow, F.S., Obbink, E.A., LeGrande, A.N., Ullman, D.J., Licciardi, J.M., 2009. Surface-melt driven Laurentide ice sheet retreat during the early

Holocene. Geophys. Res. Lett. 36 (24).

Cheng, H., Fleitmann, D., Edwards, R.L., Wang, X., Cruz, F.W., Auler, A.S., Mangini, A., Wang, Y., Kong, X., Burns, S.J., Matter, A., 2009. Timing and structure of the 8.2 kyr BP event inferred from δ18O records of stalagmites from China, Oman, and Brazil. Geology 37 (11), 1007–1010.

Clark, P.U., Marshall, S.J., Clarke, G.K., Hostetler, S.W., Licciardi, J.M., Teller, J.T., 2001. Freshwater forcing of abrupt climate change during the last glaciation. Science 293 (5528), 283–287.

Clarke, K.R., Gorley, R.N., 2006. Program Primer. Primer-E, version 6.

Clarke, G., Leverington, D., Teller, J., Dyke, A., 2003. Superlakes, megafloods, and abrupt climate change. Science 301 (5635), 922–923.

Clarke, G.K., Bush, A.B., Bush, J.W., 2009. Freshwater discharge, sediment transport, and modeled climate impacts of the final drainage of glacial Lake Agassiz. J. Clim. 22 (8), 2161–2180.

Clegg, B.F., Kelly, R., Clarke, G.H., Walker, I.R., Hu, F.S., 2011. Nonlinear response of summer temperature to Holocene insolation forcing in Alaska. Proc. Natl. Acad. Sci. 108 (48), 19299–19304.

Cranston, P.S., 1982. A Key to the Larvae of the British Orthocladiinae (Chironomidae). Freshwater Biological Association, Ambleside.

Daley, T.J., Street-Perrott, F.A., Loader, N.J., Barber, K.E., Hughes, P.D., Fisher, E.H., Marshall, J.D., 2009. Terrestrial climate signal of the "8200 yr BP cold event" in the Labrador Sea region. Geology 37 (9), 831–834.

Delworth, T.L., Zeng, F., 2016. The impact of the North Atlantic oscillation on climate through its influence on the atlantic meridional overturning circulation. J. Clim. 29 (3), 941–962.

Dixit, Y., Hodell, D.A., Sinha, R., Petrie, C.A., 2014. Abrupt weakening of the Indian summer monsoon at 8.2 kyr BP. Earth Planet. Sci. Lett. 391, 16–23.

Drijfhout, S., 2015. Competition between global warming and an abrupt collapse of the AMOC in Earth's energy imbalance. Sci. Rep. 5, 14877.

Dyke, A.S., Andrews, J.T., Clark, P.U., England, J.H., Miller, G.H., Shaw, J., Veillette, J.J., 2002. The Laurentide and Innuitian ice sheets during the last glacial maximum. Quat. Sci. Rev. 21 (1), 9–31.

Dykoski, C.A., Edwards, R.L., Cheng, H., Yuan, D., Cai, Y., Zhang, M., Lin, Y., Qing, J., An, Z., Revenaugh, J., 2005. A high-resolution, absolute-dated Holocene and deglacial Asian monsoon record from Dongge Cave, China. Earth Planet. Sci. Lett. 233 (1), 71–86.

Ecoregions Working Group, 1989. Ecoclimatic regions of Canada, first approximation. Ecol. Land Classif. Series 23.

Eggermont, H., Heiri, O., 2012. The chironomid-temperature relationship: expression in nature and palaeoenvironmental implications. Biol. Rev. 87 (2), 430–456.

Ellison, C.R., Chapman, M.R., Hall, I.R., 2006. Surface and deep ocean interactions during the cold climate event 8200 years ago. Science 312 (5782), 1929–1932.

Engels, S., Bohncke, S.J.P., Bos, J.A.A., Brooks, S.J., Heiri, O., Helmens, K.F., 2008. Chironomid-based palaeotemperature estimates for northeast Finland during oxygen isotope stage 3. J. Paleolimnol. 40 (1), 49–61.

Environment Canada, 2002. The 2002 Climate Data. CD-ROM.

Estrella-Martínez, J., Ascough, P.L., Schöne, B.R., Scourse, J.D., Butler, P.G., 2019. 8.2 ka event North Sea hydrography determined by bivalve shell stable isotope geochemistry. Sci. Rep. 9 (1), 6753.

Faegri, K., Iversen, J., 1989. In: Faegri, K., Kaland, P.E., Krzywinski, K. (Eds.), Textbook of Pollen Analysis, fourth ed.

Finkelstein, S.A., Gajewski, K., 2007. A palaeolimnological record of diatom-community dynamics and late-Holocene climatic changes from Prescott Island, Nunavut, central Canadian Arctic. Holocene 17 (6), 803–812.

Flanner, M.G., Shell, K.M., Barlage, M., Perovich, D.K., Tschudi, M.A., 2011. Radiative forcing and albedo feedback from the Northern Hemisphere cryosphere between 1979 and 2008. Nat. Geosci. 4 (3), 151–155.

Fleitmann, D., Mudelsee, M., Burns, S.J., Bradley, R.S., Kramers, J., Matter, A., 2008. Evidence for a widespread climatic anomaly at around 9.2 ka before present. Paleoceanography 23 (1).

Fortin, M.C., Medeiros, A.S., Gajewski, K., Barley, E.M., Larocque-Tobler, I., Porinchu, D.F., Wilson, S.E., 2015. Chironomid-environment relations in northern North America. J. Paleolimnol. 54 (2–3), 223–237.

Francis, D.R., 2001. A record of hypolimnetic oxygen conditions in a temperate multi-depression lake from chemical evidence and chronomid remains. J. Paleolimnol. 25 (3), 351–365.

Frey, K.E., McClelland, J.W., 2009. Impacts of permafrost degradation on arctic river biogeochemistry. Hydrol. Process. 23 (1), 169–182.

Gajewski, K., 2015. Quantitative reconstruction of Holocene temperatures across the Canadian Arctic and Greenland. Glob. Planet. Chang. 128, 14–23.

Gavin, D.G., Henderson, A.C., Westover, K.S., Fritz, S.C., Walker, I.R., Leng, M.J., Hu, F.S., 2011. Abrupt Holocene climate change and potential response to solar forcing in western Canada. Quat. Sci. Rev. 30 (9), 1243–1255.

Gregoire, L.J., Payne, A.J., Valdes, P.J., 2012. Deglacial rapid sea level rises caused by ice-sheet saddle collapses. Nature 487 (7406), 219–222.

Grimm, E.C., 1990. TILIA* GRAPH. PC spreadsheet and graphics software for pollen data. In: INQUA, Working Group on Data-Handling Methods, pp. 5–7.

Hansen, J., Sato, M., Hearty, P., Ruedy, R., Kelley, M., Masson-Delmotte, V., Russell, G., Tselioudis, G., Cao, J., Rignot, E., Velicogna, I., 2016. Ice melt, sea level rise and superstorms: evidence from paleoclimate data, climate modeling, and modern observations that 2 C global warming could be dangerous. Atmos. Chem. Phys. 16 (6), 3761–3812.

Harning, D.J., Geirsdóttir, Á., Miller, G.H., 2018. Punctuated Holocene climate of Vestfirðir, Iceland, linked to internal/external variables and oceanographic

conditions. Quat. Sci. Rev. 189, 31—42.

Hawkins, E., Smith, R.S., Allison, L.C., Gregory, J.M., Woollings, T.J., Pohlmann, H., De Cuevas, B., 2011. Bistability of the Atlantic overturning circulation in a global climate model and links to ocean freshwater transport. Geophys. Res. Lett. 38 (10).

Heiri, O., 2004. Within-lake variability of subfossil chironomid assemblages in shallow Norwegian lakes. J. Paleolimnol. 32 (1), 67—84.

Heiri, O., Lotter, A.F., 2001. Effect of low count sums on quantitative environmental reconstructions: an example using subfossil chironomids. J. Paleolimnol. 26 (3), 343—350.

Heiri, O., Lotter, A.F., Lemcke, G., 2001. Loss on ignition as a method for estimating organic and carbonate content in sediments: reproducibility and comparability of results. J. Paleolimnol. 25 (1), 101—110.

Hill, M.O., 1973. Diversity and evenness: a unifying notation and its consequences. Ecology 54 (2), 427—432.

Hobbie, J.E., Shaver, G.R., Rastetter, E.B., Cherry, J.E., Goetz, S.J., Guay, K.C., Gould, W.A., Kling, G.W., 2017. Ecosystem responses to climate change at a Low Arctic and a High Arctic long-term research site. Ambio 46 (1), 160—173.

Hoffman, J.S., Carlson, A.E., Winsor, K., Klinkhammer, G.P., LeGrande, A.N., Andrews, J.T., Strasser, J.C., 2012. Linking the 8.2 ka event and its freshwater forcing in the Labrador Sea. Geophys. Res. Lett. 39 (18).

Hofmann, M., Rahmstorf, S., 2009. On the stability of the Atlantic meridional overturning circulation. Proc. Natl. Acad. Sci. pnas-0909146106.

Hou, J., Huang, Y., Shuman, B.N., Oswald, W.W., Foster, D.R., 2012. Abrupt cooling repeatedly punctuated early-Holocene climate in eastern North America. Holocene 22 (5), 525—529.

Hu, F.S., Slawinski, D., Wright, H.E., Ito, E., Johnson, R.G., Kelts, K.R., McEwan, R.F., Boedigheimer, A., 1999. Abrupt changes in North American climate during early Holocene times. Nature 400 (6743), 437—440.

Hu, F.S., Higuera, P.E., Duffy, P., Chipman, M.L., Rocha, A.V., Young, A.M., Kelly, R., Dietze, M.C., 2015. Arctic tundra fires: natural variability and responses to climate change. Front. Ecol. Environ. 13 (7), 369—377.

Hughen, K.A., Southon, J.R., Lehman, S.J., Overpeck, J.T., 2000. Synchronous radio-carbon and climate shifts during the last deglaciation. Science 290 (5498), 1951—1954.

Huntley, B., 2012. Reconstructing palaeoclimates from biological proxies: some often overlooked sources of uncertainty. Quat. Sci. Rev. 31, 1—16.

IPCC, 2013. IPCC, 2013: Climate Change 2013: the Physical Science Basis. Contribution of Working Group I to the Fifth Assessment Report of the Intergovernmental Panel on Climate Change.

Jackson, L.C., Kahana, R., Graham, T., Ringer, M.A., Woollings, T., Mecking, J.V., Wood, R.A., 2015. Global and European climate impacts of a slowdown of the AMOC in a high resolution GCM. Clim. Dyn. 45 (11—12), 3299—3316.

Juggins, S., 1992. ZONE (Version 1.2): an MSDOS Program for Transformation and Zonation of Palaeoecological Data. University of Newcastle.

Juggins, S., 2003. Program C2 Data Analysis. University of Newcastle, Newcastle, UK.

Juggins, S., 2013. Quantitative reconstructions in palaeolimnology: new paradigm or sick science? Quat. Sci. Rev. 64, 20—32.

Juggins, S., Birks, H.J.B., 2012. Quantitative environmental reconstructions from biological data. In: Tracking Environmental Change Using Lake Sediments. Springer, Dordrecht, pp. 431—494.

Kaufman, D.S., Ager, T.A., Anderson, N.J., Anderson, P.M., Andrews, J.T., Bartlein, P.J., Brubaker, L.B., Coats, L.L., Cwynar, L.C., Duvall, M.L., Dyke, A.S., 2004. Holocene thermal maximum in the western Arctic (0—180 W). Quat. Sci. Rev. 23 (5), 529—560.

Kaufman, D.S., Axford, Y.L., Henderson, A.C., McKay, N.P., Oswald, W.W., Saenger, C., Anderson, R.S., Bailey, H.L., Clegg, B., Gajewski, K., Hu, F.S., 2016. Holocene climate changes in eastern Beringia (NW North America)—A systematic review of multi-proxy evidence. Quat. Sci. Rev. 147, 312—339.

Keigwin, L.D., Sachs, J.P., Rosenthal, Y., Boyle, E.A., 2005. The 8200 year BP event in the slope water system, western subpolar North Atlantic. Paleoceanography 20 (2).

Kobashi, T., Severinghaus, J.P., Brook, E.J., Barnola, J.M., Grachev, A.M., 2007. Precise timing and characterization of abrupt climate change 8200 years ago from air trapped in polar ice. Quat. Sci. Rev. 26 (9), 1212—1222.

Lamoureux, S., 2000. Five centuries of interannual sediment yield and rainfall-induced erosion in the Canadian High Arctic recorded in lacustrine varves. Water Resour. Res. 36 (1), 309—318.

Lamoureux, S.F., Stewart, K.A., Forbes, A.C., Fortin, D., 2006. Multidecadal variations and decline in spring discharge in the Canadian middle Arctic since 1550 AD. Geophys. Res. Lett. 33 (2).

Larocque, I., Rolland, N., 2006. A Visual Guide to Sub-fossil Chironomids from Quebec to Ellesmere Island. Rapport R-900. Institut National de la Recherche Scientifique, Québec.

Larocque, I., Pienitz, R., Rolland, N., 2006. Factors influencing the distribution of chironomids in lakes distributed along a latitudinal gradient in northwestern Quebec, Canada. Can. J. Fish. Aquat. Sci. 63 (6), 1286—1297.

Lecavalier, B.S., Fisher, D.A., Milne, G.A., Vinther, B.M., Tarasov, L., Huybrechts, P., Lacelle, D., Main, B., Zheng, J., Bourgeois, J., Dyke, A.S., 2017. High Arctic Holocene temperature record from the Agassiz ice cap and Greenland ice sheet evolution. In: Proceedings of the National Academy of Sciences, p. 201616287.

LeGrande, A.N., Schmidt, G.A., Shindell, D.T., Field, C.V., Miller, R.L., Koch, D.M., Faluvegi, G., Hoffmann, G., 2006. Consistent simulations of multiple proxy responses to an abrupt climate change event. Proc. Natl. Acad. Sci. U.S.A. 103 (4), 837—842.

Lewis, C.F.M., Miller, A.A.L., Levac, E., Piper, D.J.W., Sonnichsen, G.V., 2012. Lake Agassiz outburst age and routing by Labrador Current and the 8.2 cal ka cold event. Quat. Int. 260, 83—97.

Liu, Y.H., Henderson, G.M., Hu, C.Y., Mason, A.J., Charnley, N., Johnson, K.R., Xie, S.C., 2013. Links between the east asian monsoon and North Atlantic climate during the 8,200 year event. Nat. Geosci. 6 (2), 117—120.

Liu, W., Xie, S.P., Liu, Z., Zhu, J., 2017. Overlooked possibility of a collapsed atlantic meridional overturning circulation in warming climate. Sci. Adv. 3 (1), e1601666.

Masson-Delmotte, V., Landais, A., Stievenard, M., Cattani, O., Falourd, S., Jouzel, J., Johnsen, S.J., Dahl-Jensen, D., Sveinsbjornsdottir, A., White, J.W.C., Popp, T., 2005. Holocene climatic changes in Greenland: different deuterium excess signals at Greenland ice core project (GRIP) and NorthGRIP. J. Geophys. Res.: Atmospheres 110 (D14).

MacDonald, G.M., Porinchu, D.F., Rolland, N., Kremenetsky, K.V., Kaufman, D.S., 2009. Paleolimnological evidence of the response of the central Canadian treeline zone to radiative forcing and hemispheric patterns of temperature change over the past 2000 years. J. Paleolimnol. 41 (1), 129—141.

Mahajan, S., Zhang, R., Delworth, T.L., 2011. Impact of the Atlantic meridional overturning circulation (AMOC) on Arctic surface air temperature and sea ice variability. J. Clim. 24 (24), 6573—6581.

Maher, L.J., 1972. Nomograms for computing 0.95 confidence limits of pollen data. Rev. Palaeobot. Palynol. 13 (2), 85—93.

Matero, I.S.O., Gregoire, L.J., Ivanovic, R.F., Tindall, J.C., Haywood, A.M., 2017. The 8.2 ka cooling event caused by Laurentide ice saddle collapse. Earth Planet. Sci. Lett. 473, 205—214.

McAndrews, J.H., 1984. Pollen analysis of the 1973 ice core from Devon Island glacier, Canada. Quat. Res. 22 (1), 68—76.

Medeiros, A.S., Gajewski, K., Porinchu, D.F., Vermaire, J.C., Wolfe, B.B., 2015. Detecting the influence of secondary environmental gradients on chironomid-inferred paleotemperature reconstructions in northern North America. Quat. Sci. Rev. 124, 265—274.

Mikolajewicz, U., Crowley, T.J., Schiller, A., Voss, R., 1997. Modelling teleconnections between the North Atlantic and north Pacific during the younger dryas. Nature 387 (6631), 384.

Moossen, H., Bendle, J., Seki, O., Quillmann, U., Kawamura, K., 2015. North Atlantic Holocene climate evolution recorded by high-resolution terrestrial and marine biomarker records. Quat. Sci. Rev. 129, 111—127.

Morrill, C., Jacobsen, R.M., 2005. How widespread were climate anomalies 8200 years ago? Geophys. Res. Lett. 32 (19).

Morrill, C., LeGrande, A.N., Renssen, H., Bakker, P., Otto-Bliesner, B.L., 2013. Model sensitivity to North Atlantic freshwater forcing at 8.2 ka. Clim. Past 9 (2), 955—968.

North Greenland Ice Core Project (NGRIP), 2004. High-resolution record of Northern Hemisphere climate extending into the last interglacial period. Nature 431 (7005), 147—151.

Notz, D., Stroeve, J., 2016. Observed Arctic sea-ice loss directly follows anthropogenic CO2 emission. Science 354 (6313), 747—750.

Olander, H., Birks, H.J.B., Korhola, A., Blom, T., 1999. An expanded calibration model for inferring lake water and air temperatures from fossil chironomid assemblages in northern Fennoscandia. Holocene 9 (3), 279—294.

Oliver, D.R., Roussel, M.E., 1983. The Insects and Arachnids of Canada. Part 11. The Genera of Larval Midges of Canada. Diptera: Chironomidae. Minister of Supply and Services.

Olson, R., An, S.I., Fan, Y., Evans, J.P., Caesar, L., 2018. North Atlantic observations sharpen meridional overturning projections. Clim. Dyn. 50 (11—12), 4171—4188.

Paul, C.A., Rühland, K.M., Smol, J.P., 2010. Diatom-inferred climatic and environmental changes over the last~ 9000 years from a low Arctic (Nunavut, Canada) tundra lake. Palaeogeogr. Palaeoclimatol. Palaeoecol. 291 (3), 205—216.

Pecl, G.T., Araújo, M.B., Bell, J.D., Blanchard, J., Bonebrake, T.C., Chen, I.C., Clark, T.D., Colwell, R.K., Danielsen, F., Evengård, B., Falconi, L., 2017. Biodiversity redistribution under climate change: impacts on ecosystems and human well-being. Science 355 (6332), 9214.

Peros, M.C., Gajewski, K., 2009. Pollen-based reconstructions of late Holocene climate from the central and western Canadian Arctic. J. Paleolimnol. 41 (1), 161—175.

Porinchu, D.F., Cwynar, L.C., 2002. Late-Quaternary history of midge communities and climate from a tundra site near the lower Lena River, Northeast Siberia. J. Paleolimnol. 27 (1), 59—69.

Porinchu, D.F., MacDonald, G.M., 2003. The use and application of freshwater midges (Chironomidae: Insecta: Diptera) in geographical research. Prog. Phys. Geogr. 27 (3), 378—422.

Porinchu, D., Rolland, N., Moser, K., 2009a. Development of a chironomid-based air temperature inference model for the central Canadian Arctic. J. Paleolimnol. 41 (2), 349—368.

Porinchu, D.F., MacDonald, G.M., Rolland, N., 2009b. A 2000 year midge-based paleotemperature reconstruction from the Canadian Arctic archipelago. J. Paleolimnol. 41 (1), 177—188.

Potapova, M.G., Ponader, K.C., Lowe, R.L., Clason, T.A., Bahls, L.L., 2003. Small-celled Nupela species from north America. Diatom Res. 18 (2), 293—306.

Rahmstorf, S., 1995. Bifurcations of the Atlantic thermohaline circulation in response to changes in the hydrological cycle. Nature 378 (6553), 145.

Rahmstorf, S., 2002. Ocean circulation and climate during the past 120,000 years. Nature 419 (6903), 207.

Rahmstorf, S., Box, J.E., Feulner, G., Mann, M.E., Robinson, A., Rutherford, S.,

Schaffernicht, E.J., 2015. Exceptional twentieth-century slowdown in Atlantic Ocean overturning circulation. Nat. Clim. Chang. 5 (5), 475.

Rasmussen, S.O., Vinther, B.M., Clausen, H.B., Andersen, K.K., 2007. Early Holocene climate oscillations recorded in three Greenland ice cores. Quat. Sci. Rev. 26 (15), 1907—1914.

Reimer, P.J., Bard, E., Bayliss, A., Beck, J.W., Blackwell, P.G., Ramsey, C.B., Buck, C.E., Cheng, H., Edwards, R.L., Friedrich, M., Grootes, P.M., 2013. IntCal13 and Marine 13 radiocarbon age calibration curves 0—50,000 years cal BP. Radiocarbon 55 (4), 1869—1887.

Rind, D., Schmidt, G.A., Jonas, J., Miller, R., Nazarenko, L., Kelley, M., Romanski, J., 2018. Multicentury instability of the Atlantic meridional circulation in rapid warming simulations with GISS ModelE2. J. Geophys. Res.: Atmospheres 123 (12), 6331—6355.

Rohling, E.J., Pälike, H., 2005. Centennial-scale climate cooling with a sudden cold event around 8,200 years ago. Nature 434 (7036), 975—979.

Rolland, N., Larocque, I., Francus, P., Pienitz, R., Laperrière, L., 2008. Holocene climate inferred from biological (Diptera: Chironomidae) analyses in a Southampton Island (Nunavut, Canada) lake. Holocene 18 (2), 229—241.

Romanovsky, V., Burgess, M., Smith, S., Yoshikawa, K., Brown, J., 2002. Permafrost temperature records: indicators of climate change. EOS Trans. Am. Geophys. Union 83 (50), 589—594.

Rosén, P., Hall, R., Korsman, T., Renberg, I., 2000. Diatom transfer-functions for quantifying past air temperature, pH and total organic carbon concentration from lakes in northern Sweden. J. Paleolimnol. 24 (2), 109—123.

Rühland, K., Paterson, A.M., Smol, J.P., 2008. Hemispheric-scale patterns of climate-related shifts in planktonic diatoms from North American and European lakes. Glob. Chang. Biol. 14 (11), 2740—2754.

Rühland, K.M., Paterson, A.M., Smol, J.P., 2015. Lake diatom responses to warming: reviewing the evidence. J. Paleolimnol. 54, 1—35.

Schmittner, A., Latif, M., Schneider, B., 2005. Model projections of the North Atlantic thermohaline circulation for the 21st century assessed by observations. Geophys. Res. Lett. 32 (23).

Schuur, E.A., McGuire, A.D., Schädel, C., Grosse, G., Harden, J.W., Hayes, D.J., Hugelius, G., Koven, C.D., Kuhry, P., Lawrence, D.M., Natali, S.M., 2015. Climate change and the permafrost carbon feedback. Nature 520 (7546), 171.

Seppä, H., Cwynar, L.C., MacDonald, G.M., 2003. Post-glacial vegetation reconstruction and a possible 8200 cal. yr BP event from the low arctic of continental Nunavut, Canada. J. Quat. Sci. 18 (7), 621—629.

Seppä, H., Birks, H.J.B., Giesecke, T., Hammarlund, D., Alenius, T., Antonsson, K., Bjune, A.E., Heikkilä, M., MacDonald, G.M., Ojala, A.E.K., Telford, R.J., 2007. Spatial structure of the 8200 cal yr BP event in northern Europe. Clim. Past Discuss. 3 (1), 165—195.

Seppä, H., Bjune, A.E., Telford, R.J., Birks, H.J.B., Veski, S., 2009. Last nine-thousand years of temperature variability in Northern Europe. Clim. Past 5 (3), 523—535.

Shuman, B., 2003. Controls on loss-on-ignition variation in cores from two shallow lakes in the northeastern United States. J. Paleolimnol. 30 (4), 371—385.

Simola, H., Meriläinen, J.J., Sandman, O., Marttila, V., Karjalainen, H., Kukkonen, M., Julkunen-Tiitto, H., Hakulinen, J., 1996. Palaeolimnological analyses as information source for large lake biomonitoring. In: The First International Lake Ladoga Symposium. Springer Netherlands, pp. 283—292.

Smeed, D.A., Josey, S.A., Beaulieu, C., Johns, W.E., Moat, B.I., Frajka-Williams, E., Rayner, D., Meinen, C.S., Baringer, M.O., Bryden, H.L., McCarthy, G.D., 2018. The North Atlantic Ocean is in a state of reduced overturning. Geophys. Res. Lett. 45 (3), 1527—1533.

Smol, J.P., Douglas, M.S., 2007. Crossing the final ecological threshold in high Arctic ponds. Proc. Natl. Acad. Sci. 104 (30), 12395—12397.

Smol, J.P., Wolfe, A.P., Birks, H.J.B., Douglas, M.S., Jones, V.J., Korhola, A., Pienitz, R., Rühland, K., Sorvari, S., Antoniades, D., Brooks, S.J., 2005. Climate-driven regime shifts in the biological communities of arctic lakes. Proc. Natl. Acad. Sci. U.S.A. 102 (12), 4397—4402.

Stanek-Tarkowska, J., Wetzel, C.E., Noga, T., Ector, L., 2016. Study of the type material of Navicula egregia Hustedt and descriptions of two new aerial Microcostatus (Bacillariophyta) species from Central Europe. Phytotaxa 280 (2), 163—172.

Stockmarr, J., 1971. Tablets with spores used in absolute pollen analysis.Pollen et spores.

Stouffer, R.J., Yin, J., Gregory, J.M., Dixon, K.W., Spelman, M.J., Hurlin, W., Weaver, A.J., Eby, M., Flato, G.M., Hasumi, H., Hu, A., 2006. Investigating the causes of the response of the thermohaline circulation to past and future climate changes. J. Clim. 19 (8), 1365—1387.

Stuiver, M., Reimer, P.J., Reimer, R.W., 2019. CALIB 7.1 [WWW program] at. http://calib.org. (Accessed 12 May 2019).

Taylor, J.C., Levanets, A., Blanco, S., Ector, L., 2010. Microcostatus schoemanii sp. nov., M. cholnokyi sp. nov. and M. angloensis sp. nov. three new terrestrial diatoms (Bacillariophyceae) from South Africa. Phycol. Res. 58 (3), 177—187.

Teller, J.T., Leverington, D.W., Mann, J.D., 2002. Freshwater outbursts to the oceans from glacial Lake Agassiz and their role in climate change during the last deglaciation. Quat. Sci. Rev. 21 (8), 879—887.

ter Braak, C.J., Juggins, S., 1993. Weighted averaging partial least squares regression (WA-PLS): an improved method for reconstructing environmental variables from species assemblages. In: Twelfth International Diatom Symposium. Springer, Dordrecht, pp. 485—502.

Thibodeau, B., Not, C., Zhu, J., Schmittner, A., Noone, D., Tabor, C., Zhang, J., Liu, Z., 2018. Last century warming over the Canadian atlantic shelves linked to weak atlantic meridional overturning circulation. Geophys. Res. Lett. https://doi.org/10.1002/essoar.10500026.2.

Thomas, E.R., Wolff, E.W., Mulvaney, R., Steffensen, J.P., Johnsen, S.J., Arrowsmith, C., White, J.W., Vaughn, B., Popp, T., 2007. The 8.2 ka event from Greenland ice cores. Quat. Sci. Rev. 26 (1), 70—81.

Thornalley, D.J., Elderfield, H., McCave, I.N., 2009. Holocene oscillations in temperature and salinity of the surface subpolar North Atlantic. Nature 457 (7230), 711.

Thornalley, D.J., McCave, I.N., Elderfield, H., 2010. Freshwater input and abrupt deglacial climate change in the North Atlantic. Paleoceanography 25 (1).

Thornalley, D.J., Oppo, D.W., Ortega, P., Robson, J.I., Brierley, C.M., Davis, R., Hall, I.R., Moffa-Sanchez, P., Rose, N.L., Spooner, P.T., Yashayaev, I., 2018. Anomalously weak Labrador Sea convection and Atlantic overturning during the past 150 years. Nature 556 (7700), 227.

Törnqvist, T.E., Hijma, M.P., 2012. Links between early Holocene ice-sheet decay, sea-level rise and abrupt climate change. Nat. Geosci. 5 (9), 601—606.

Upiter, L.M., Vermaire, J.C., Patterson, R.T., Crann, C.A., Galloway, J.M., Macumber, A.L., Neville, L.A., Swindles, G.T., Falck, H., Roe, H.M., Pisaric, M.F., 2014. Middle to late Holocene chironomid-inferred July temperatures for the central northwest Territories, Canada. J. Paleolimnol. 52 (1—2), 11—26.

Velle, G., Brodersen, K.P., Birks, H.J.B., Willassen, E., 2010. Midges as quantitative temperature indicator species: lessons for palaeoecology. Holocene 20 (6), 989—1002.

Velle, G., Brodersen, K.P., Birks, H.J.B., Willassen, E., 2012. Inconsistent results should not be overlooked: a reply to Brooks et al. (2012). Holocene 22 (12), 1501—1508.

Vinther, B.M., Buchardt, S.L., Clausen, H.B., Dahl-Jensen, D., Johnsen, S.J., Fisher, D.A., Koerner, R.M., Raynaud, D., Lipenkov, V., Andersen, K.K., Blunier, T., 2009. Holocene thinning of the Greenland ice sheet. Nature 461 (7262), 385.

Voarintsoa, N.R.G., Matero, I.S., Railsback, L.B., Gregoire, L.J., Tindall, J., Sime, L., Cheng, H., Edwards, R.L., Brook, G.A., Kathayat, G., Li, X., 2019. Investigating the 8.2 ka event in northwestern Madagascar: insight from data—model comparisons. Quat. Sci. Rev. 204, 172—186.

von Grafenstein, U., Erlenkeuser, H., Brauer, A., Jouzel, J., Johnsen, S.J., 1999. A mid-European decadal isotope-climate record from 15,500 to 5000 years BP. Science 284 (5420), 1654—1657.

Wagner, A.J., Morrill, C., Otto-Bliesner, B.L., Rosenbloom, N., Watkins, K.R., 2013. Model support for forcing of the 8.2 ka event by meltwater from the Hudson Bay ice dome. Clim. Dyn. 41 (11—12), 2855—2873.

Walker, I.R., Cwynar, L.C., 2006. Midges and palaeotemperature reconstruction—the North American experience. Quat. Sci. Rev. 25 (15—16), 1911—1925.

Walker, I.R., MacDonald, G.M., 1995. Distributions of Chironomidae (Insecta: Diptera) and other freshwater midges with respect to treeline, Northwest Territories, Canada. Arct. Alp. Res. 258—263.

Walker, I.R., Smol, J.P., Engstrom, D.R., Birks, H.J.B., 1991. An assessment of Chironomidae as quantitative indicators of past climatic change. Can. J. Fish. Aquat. Sci. 48 (6), 975—987.

Walker, I.R., Levesque, A.J., Cwynar, L.C., Lotter, A.F., 1997. An expanded surface-water palaeotemperature inference model for use with fossil midges from eastern Canada. J. Paleolimnol. 18 (2), 165—178.

Wang, Y., Cheng, H., Edwards, R.L., He, Y., Kong, X., An, Z., Wu, J., Kelly, M.J., Dykoski, C.A., Li, X., 2005. The Holocene Asian monsoon: links to solar changes and North Atlantic climate. Science 308 (5723), 854—857.

Wiederholm, T., 1989. Chironomidae of the Holarctic region. Keys and diagnoses. Part 3. Adult males. Entomol. Scand. Supplement (34).

Wiersma, A.P., Renssen, H., 2006. Model—data comparison for the 8.2 ka BP event: confirmation of a forcing mechanism by catastrophic drainage of Laurentide Lakes. Quat. Sci. Rev. 25 (1), 63—88.

Wiersma, A.P., Roche, D.M., Renssen, H., 2011. Fingerprinting the 8.2 ka event climate response in a coupled climate model. J. Quat. Sci. 26 (1), 118—127.

Wright Jr., H.E., 1991. Coring tips. J. Paleolimnol. 6 (1), 37—49.

Young, N.E., Briner, J.P., Axford, Y., Csatho, B., Babonis, G.S., Rood, D.H., Finkel, R.C., 2011. Response of a marine-terminating Greenland outlet glacier to abrupt cooling 8200 and 9300 years ago. Geophys. Res. Lett. 38 (24).

Young, N.E., Briner, J.P., Rood, D.H., Finkel, R.C., Corbett, L.B., Bierman, P.R., 2013. Age of the Fjord Stade moraines in the Disko Bugt region, western Greenland, and the 9.3 and 8.2 ka cooling events. Quat. Sci. Rev. 60, 76—90.

Yu, S.Y., Colman, S.M., Lowell, T.V., Milne, G.A., Fisher, T.G., Breckenridge, A., Boyd, M., Teller, J.T., 2010. Freshwater outburst from Lake Superior as a trigger for the cold event 9300 years ago. Science 328 (5983), 1262—1266.

Zhang, W., Yan, H., Dodson, J., Cheng, P., Liu, C., Li, J., Lu, F., Zhou, W., An, Z., 2018. The 9.2 ka event in Asian summer monsoon area: the strongest millennial scale collapse of the monsoon during the Holocene. Clim. Dyn. 50 (7—8), 2767—2782.